Heavy ion collisions: tool for studying strong-interaction matter

Che-Ming Ko
Texas A&M University

- Introduction
- Deeply inelastic collisions: nuclear dissipation
- High energy collisions: nuclear equation of state
- Collisions with neutron-rich nuclei: nuclear symmetry energy
- Collisions at relativistic energies: quark-gluon plasma and exotic hadrons
- Conclusions

Mapping QCD phase diagram via heavy ion collisions

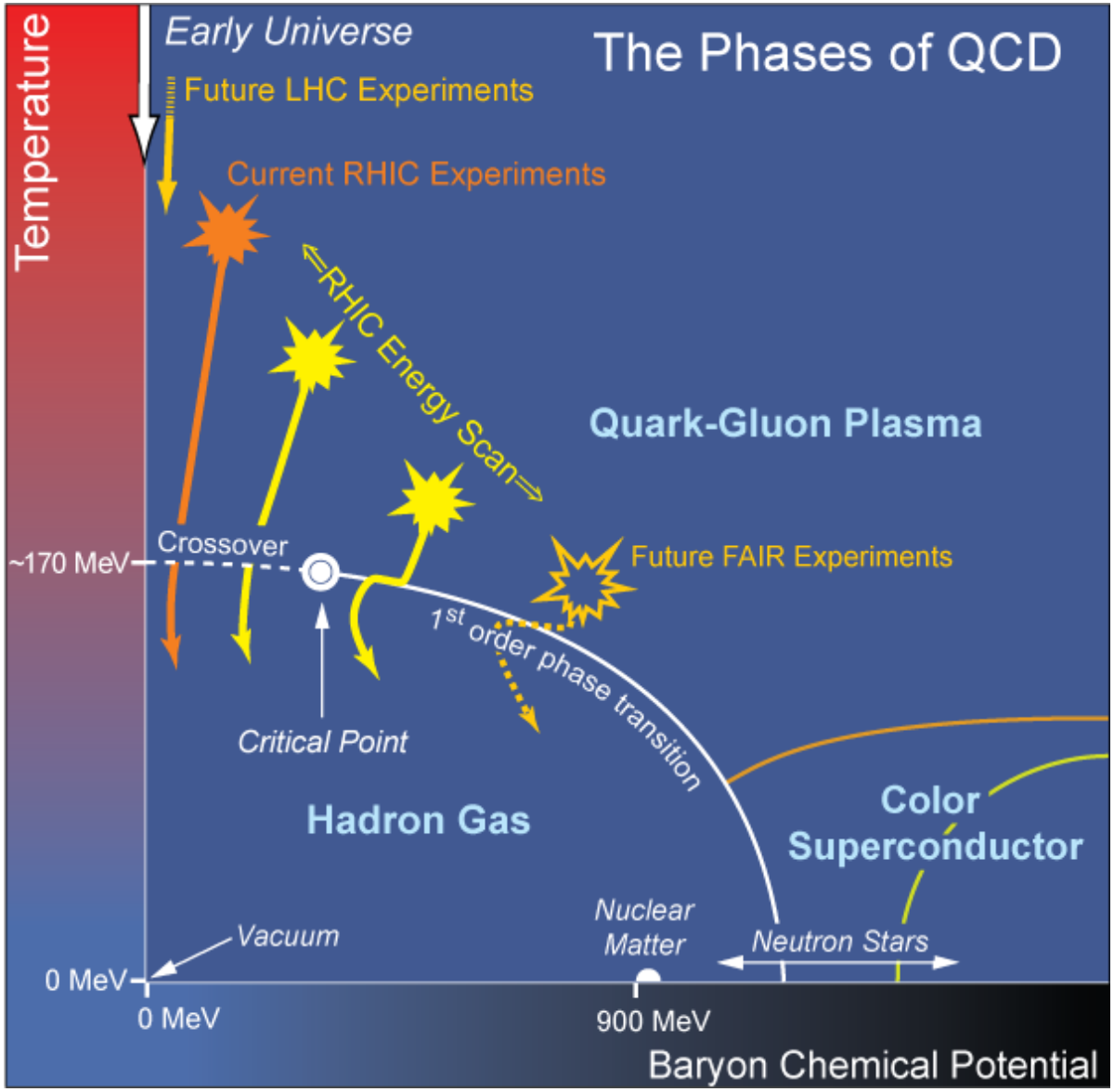

Chronology of heavy ion collisions

- 1970's: below Coulomb barrier → deeply inelastic collisions;
  nuclear dissipation and damping of collective motions
- 1980's: high energies (~1-2 GeV/nucleon @ fixed target, Bevalac);
  nuclear equation of state at high densities (~$3\rho_0$)
- 1990's: high (GSI) and relativistic (~10-100 GeV/nucleon @ fixed target, AGS, SPS);
  nuclear equation of state (~$5\rho_0$) and quark-gluon plasma
- 2000's: ultrarelativistic energies (~100-200 GeV/nucleon @ c.m., RHIC)
  → nearly baryon-free quark-gluon plasma;
  neutron-rich nuclei (MSU,GSI) → nuclear symmetry energy (~ρ_0)
- 2010's: ultrarelativstic energies (~5 TeV/nucleon @ c.m., LHC)
  → baryon-free quark-gluon plasma
- 2020's: relativistic energies (~10 GeV/nucleon @ c.m., FAIR)
  → baryon-rich quark-gluon plasma;
  medium energies (~ 250 MeV/nucleon @ fixed target, FRIB)
  → nuclear symmetry energy (~$2.5\rho_0$)

Heavy ion deeply inelastic collisions

Wilczynski, PLB 47, 484 (1973)

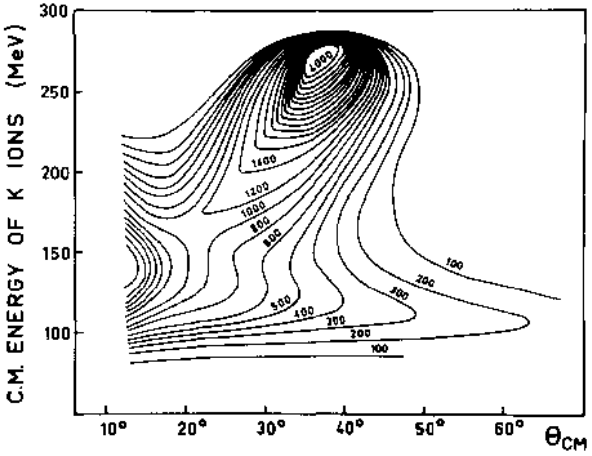

Fig. 1. Contour map of the differential cross section $(d^2\sigma/dE \cdot d\theta)_{CM}$ (in μb/MeV · rad) in the reaction ^{232}Th(^{40}Ar, K) at E_{lab} = 388 MeV, as a function of the scattering angle θ_{CM} and the C.M. energy of the detected K ions.

Devi et al. PRC 23, 1064 (1981)

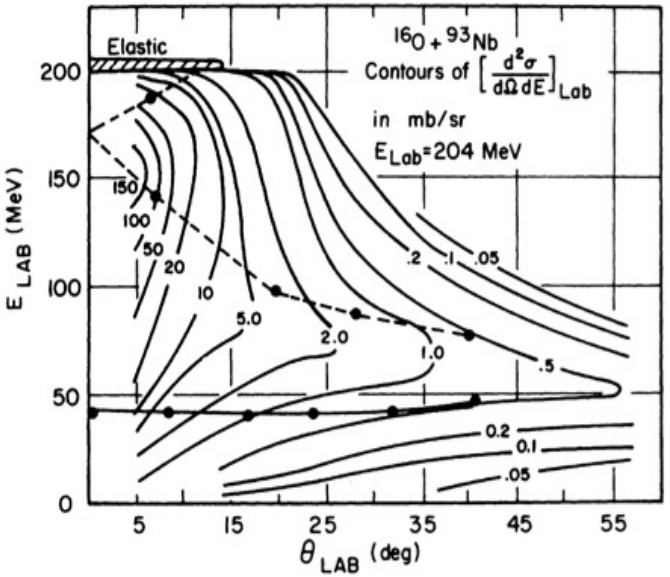

Agassi, Weidenmuller & Ko, PLB 73, 285 (1978)

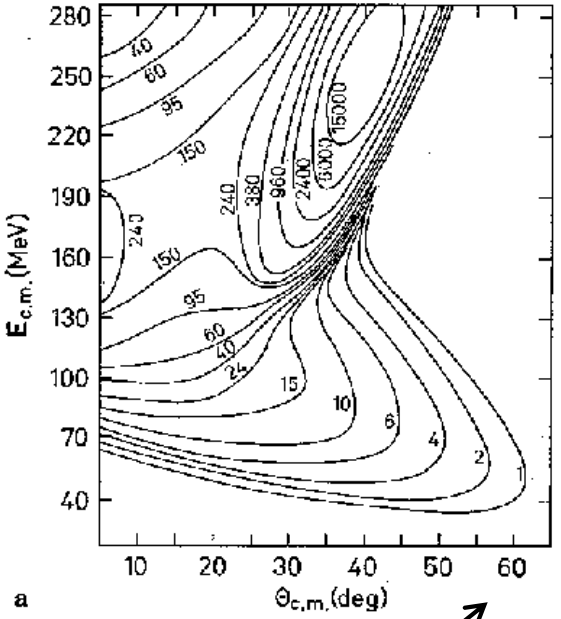

- Time-dependent Hartree-Fock (TDHF) can describe the average behavior of HI deeply inelastic collisions.
- Needs inclusion of fluctuation effect on relative motion to better describe the data.

- Transport model reasonably describes the data → energy loss of about 15 MeV/fm.
- Including other collective degrees of freedom, e.g., deformation, improves the results. (Ko, PLB 81, 299 (1979).

Nuclear symmetry energy

Li, Chen & Ko, Phys. Rep. 464, 113 (2008)

EOS of asymmetric nuclear matter

$$E(\rho,\delta) \approx E(\rho,\delta=0) + E_{sym}(\rho)\delta^2, \quad \delta = \frac{\rho_n - \rho_p}{\rho_n + \rho_p}$$

Symmetry energy

$$E_{sym}(\rho) = E_{sym}(\rho_0) + L\left(\frac{\rho-\rho_0}{3\rho_0}\right) + \frac{K_{sym}}{2}\left(\frac{\rho-\rho_0}{3\rho_0}\right)^2 + \frac{J_{sym}}{3}\left(\frac{\rho-\rho_0}{3\rho_0}\right)^3 \cdots$$

Symmetry energy coefficient $E_{sym}(\rho_0) \approx 30$ MeV from mass formula

Slope $L = 3\rho_0 \left.\frac{\partial E_{sym}(\rho)}{\partial \rho}\right|_{\rho=\rho_0}$ theoretical values -50 to 200 MeV

Curvature $K_{sym} = 9\rho_0^2 \left.\frac{\partial^2 E_{sym}(\rho)}{\partial^2 \rho}\right|_{\rho=\rho_0}$ theoretical values -700 to 466 MeV

Nuclear matter Incompressibility $K(\delta) = K_0 + K_{asy}\delta^2, \quad K_{asy} = K_{sym} - 6L$

Empirically, $K_0 \sim 230 \pm 10$ MeV, $K_{asy} \sim -500 \pm 50$ MeV, $L \sim 88 \pm 50$ MeV

$E_{sym}(\rho) \sim 32\,(\rho/\rho_0)^{\gamma}$ with $0.7 < \gamma < 1.1$ for $\rho < 1.2\rho_0$

- Symmetry energy at high densities is practically undetermined !

Equation of state of symmetric nuclear matter

Li, Machleidt & Brockmann, PRC 45, 2782 (1992)

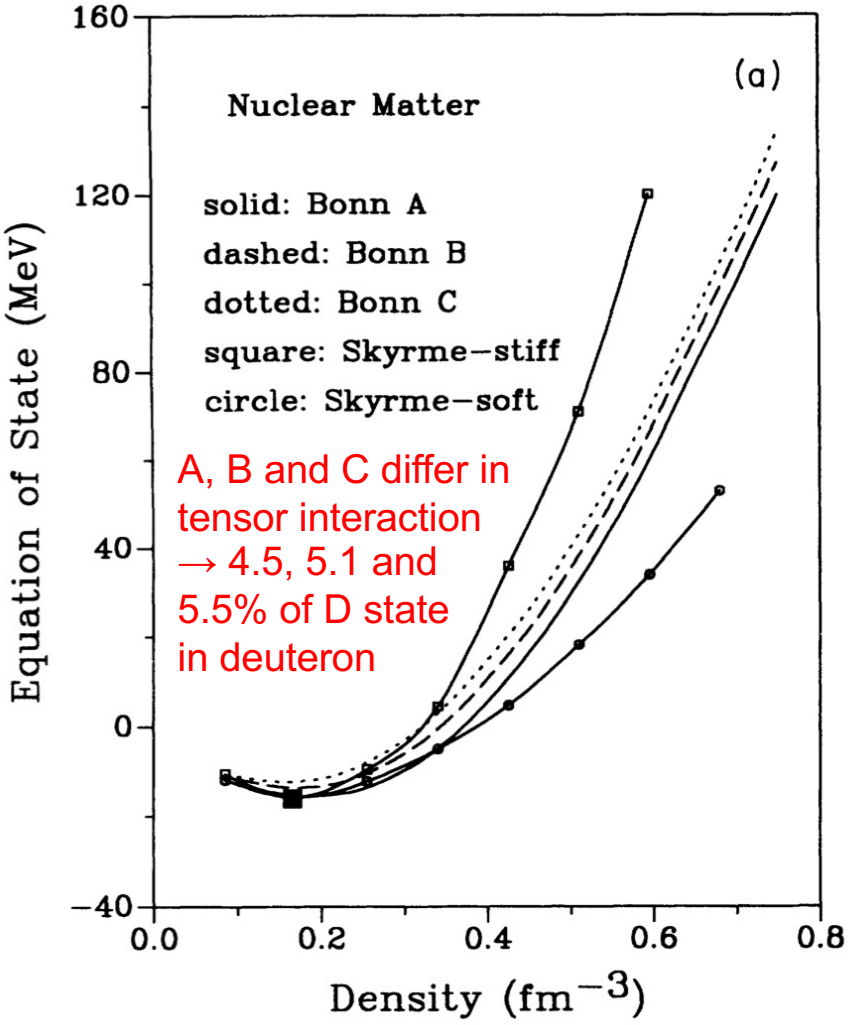

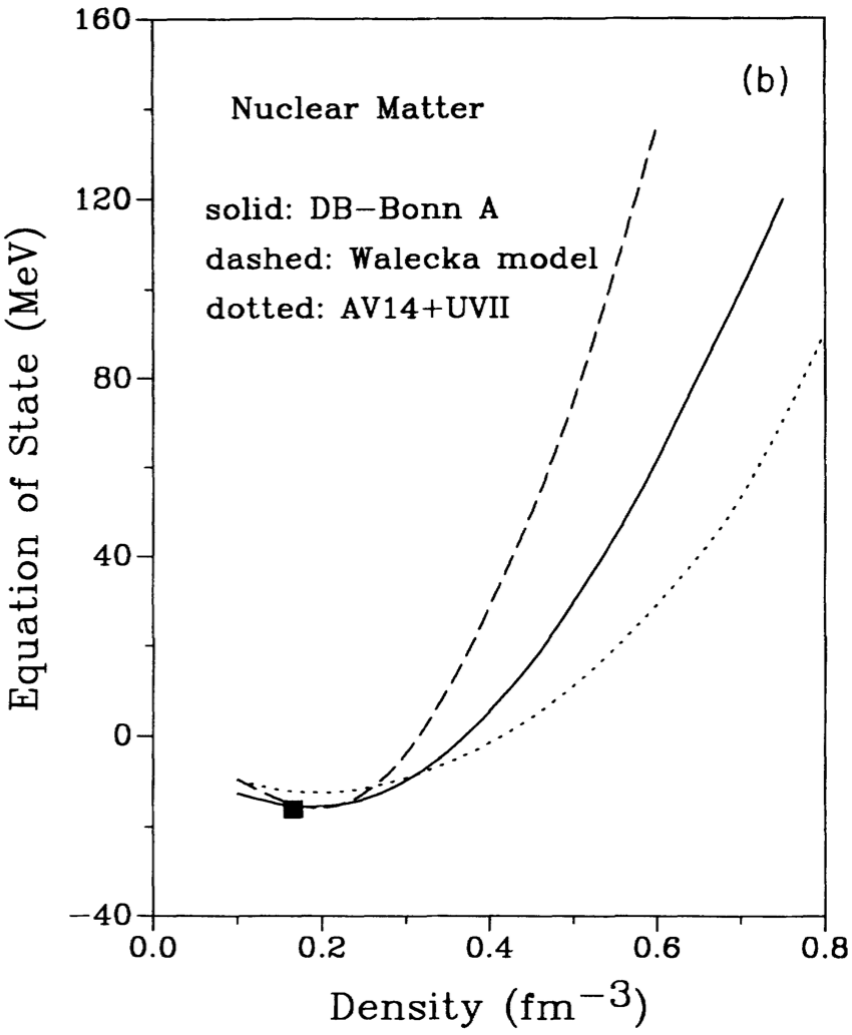

- Large uncertainties at high densities or in the stiffness of nuclear matter equation of state

Boltzmann-Uehling-Uhlenbeck model

Bertsch & Das Gupta, Phys. Rep. 160, 189 (1988)

$$\frac{\partial f(r,p,t)}{\partial t} + v\cdot\nabla_r f - \nabla_r U\cdot\nabla_p f = \left(\frac{\partial f}{\partial t}\right)_{coll}$$

$$= \frac{4}{(2\pi)^3}\iint dp_2 dp_3 \int d\Omega |v_{12}| \frac{d\sigma}{d\Omega}(p_2 - p_4)\delta(p + p_2 - p_3 - p_4)$$

$$\times\{f(r,p_3,t)f(r,p_4,t)[1-f(r,p,t)][1-f(r,p_2,t)]$$

$$- f(r,p,t)f(r,p_2,t)[1-f(r,p_3,t)][1-f(r,p_4,t)]\}$$

- F(r,p,t): nucleon distribution function
- U(r): nuclear mean-field potential

  e.g., Skyrme potential $U=\alpha\,\rho(r) + \beta\,\rho^{4/3}(r)$
- $d\sigma/d\Omega$: nucleon-nucleon scattering cross sections

Collective flow in heavy ion collisions

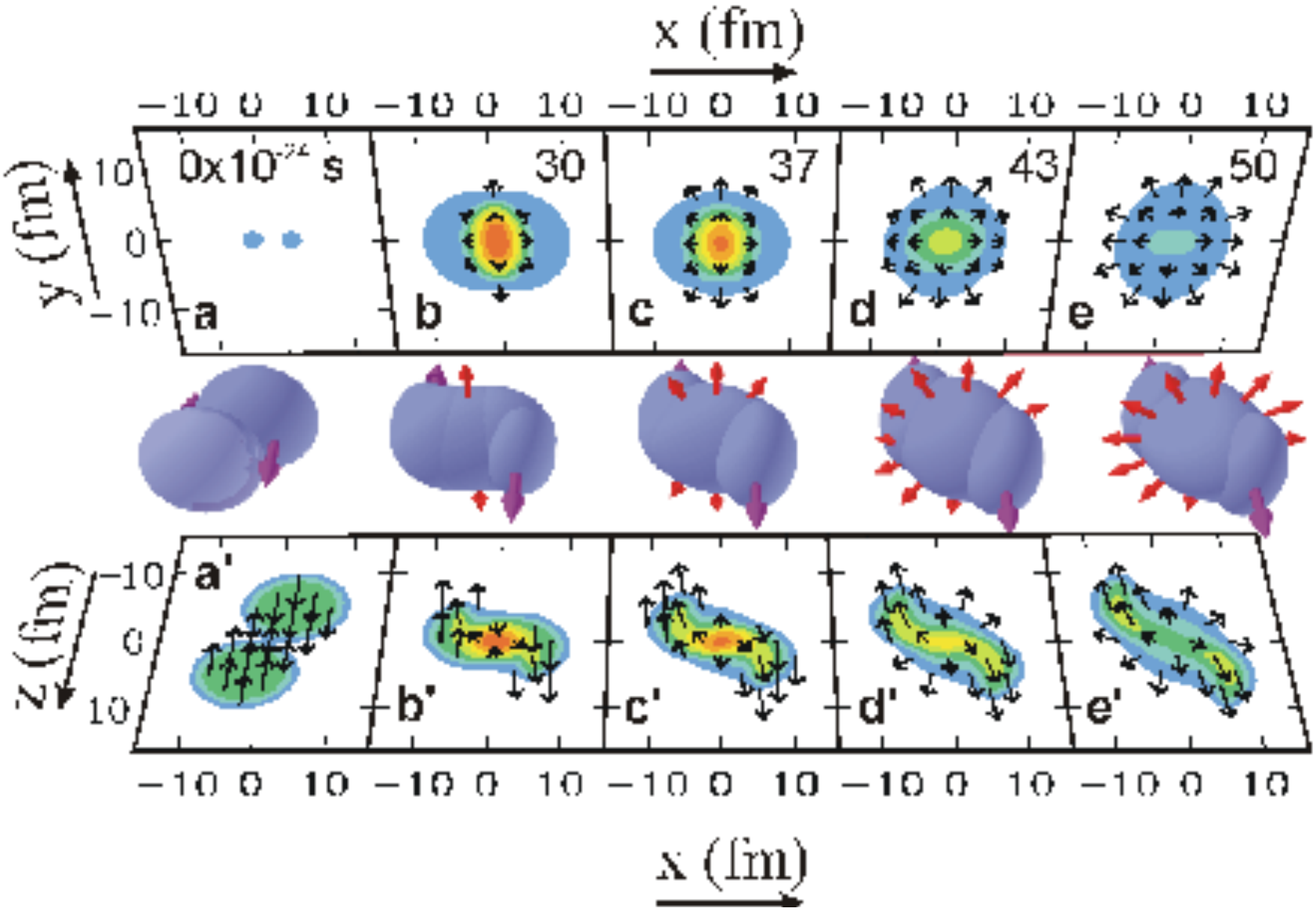

- Directed flow in the reaction (x-z) plane and elliptic flow in the transverse (x-y) plane.

Anisotropic flow

Anisotropic flow v_n

$$E\frac{d^3N}{d^3\vec{p}} = \frac{dN}{p_T dp_T d\varphi dy} = \frac{1}{2\pi}\frac{dN}{p_T dp_T dy}\left[1+\sum_{n=1}^{\infty} 2v_n(p_T, y)\cos(n\varphi)\right]$$

Sine terms vanish because of the symmetry Φ ➔ -Φ in A+A collisions

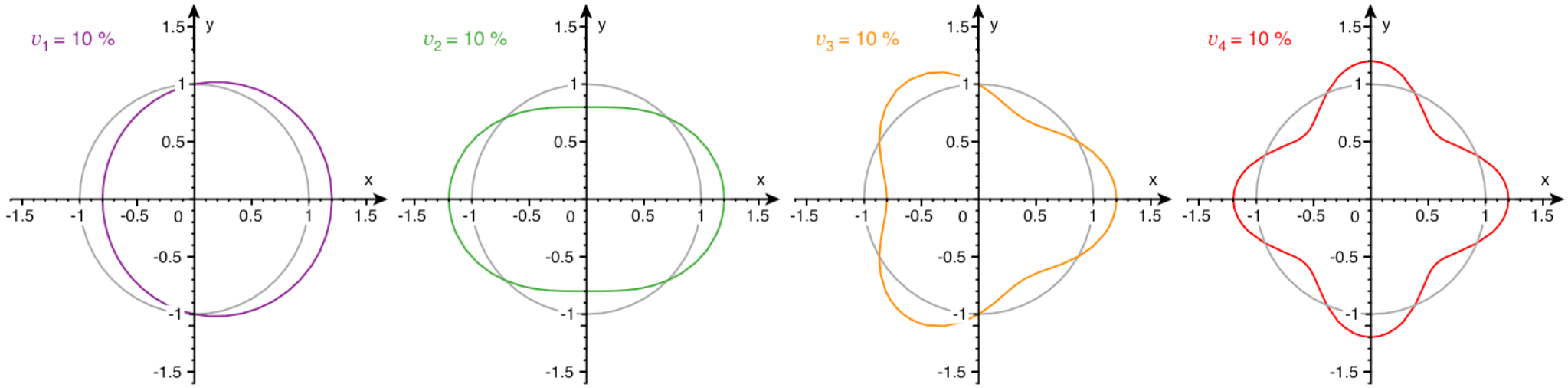

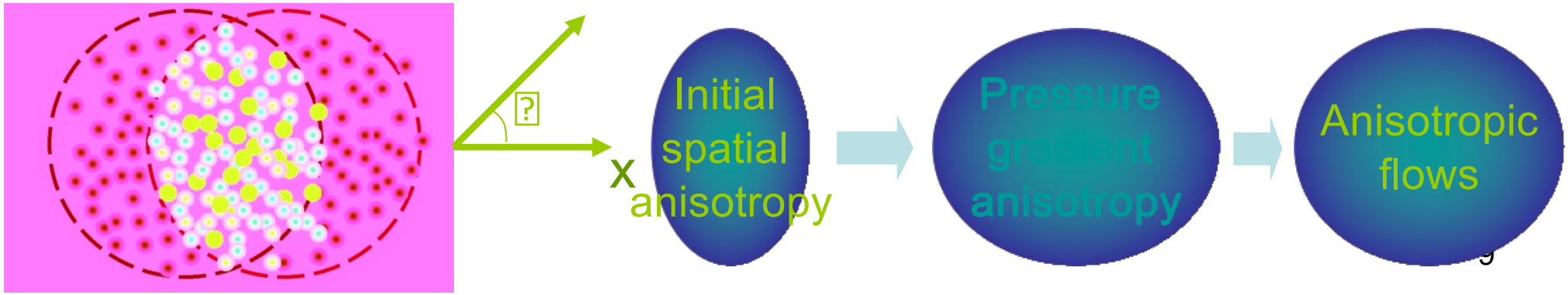

Direct and elliptic flows

Danielewicz, Lacey & Lynch, Science 298, 1592 (2002)

Direct flow $F = \left(\frac{dp_x}{dy} \right)_{y_{cm}}$

Elliptic flow $v_2 = \langle \cos 2\varphi \rangle = \left\langle \frac{p_x^2 - p_y^2}{p_x^2 + p_y^2} \right\rangle$

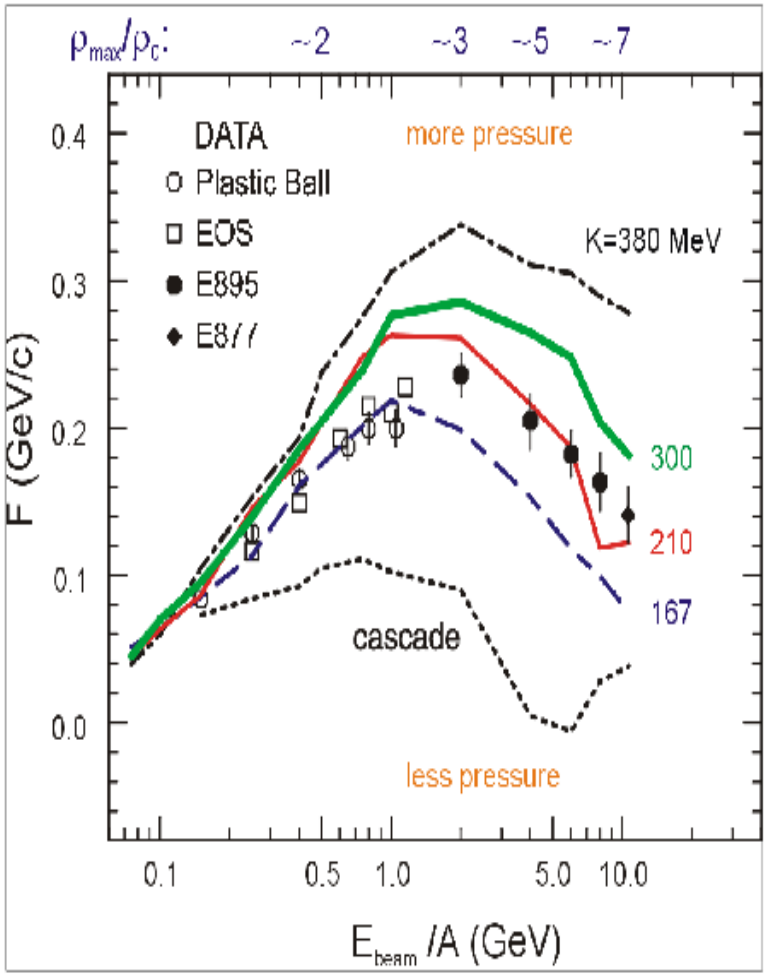

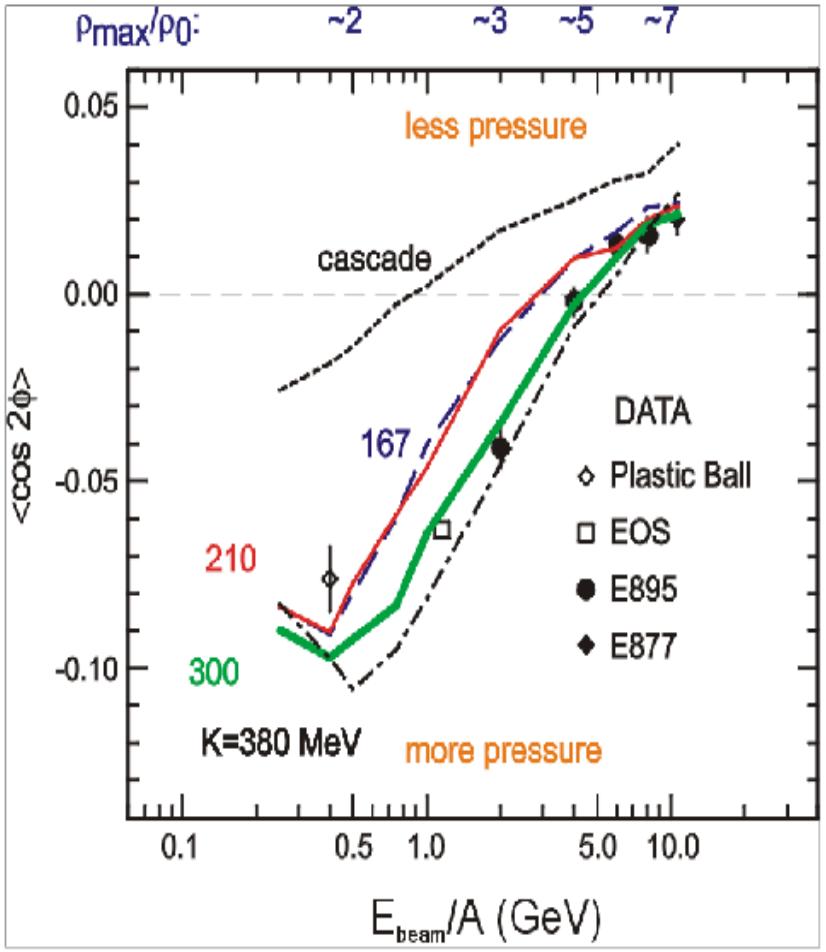

$$E_0(\rho) = E_0(\rho_0) + \frac{K_0}{2}\left(\frac{\rho - \rho_0}{3\rho_0}\right)^2 + \frac{J_0}{6}\left(\frac{\rho - \rho_0}{3\rho_0}\right)^3$$

- Data consistent with a nuclear EOS with $K_0 \approx 200$ - 300 MeV.

Subthreshold kaon production

Aichelin & Ko, PRL 55, 2661 (1985)

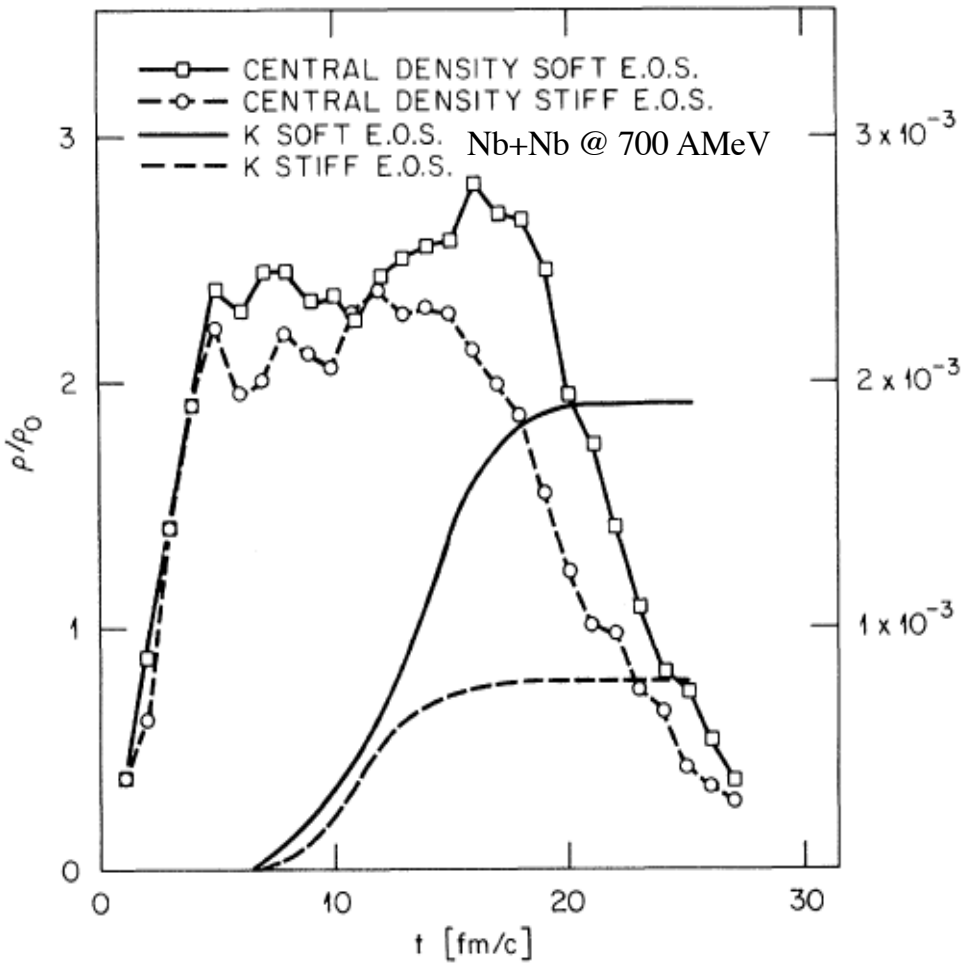

Fuchs, PRL 86, 1974 (2001)

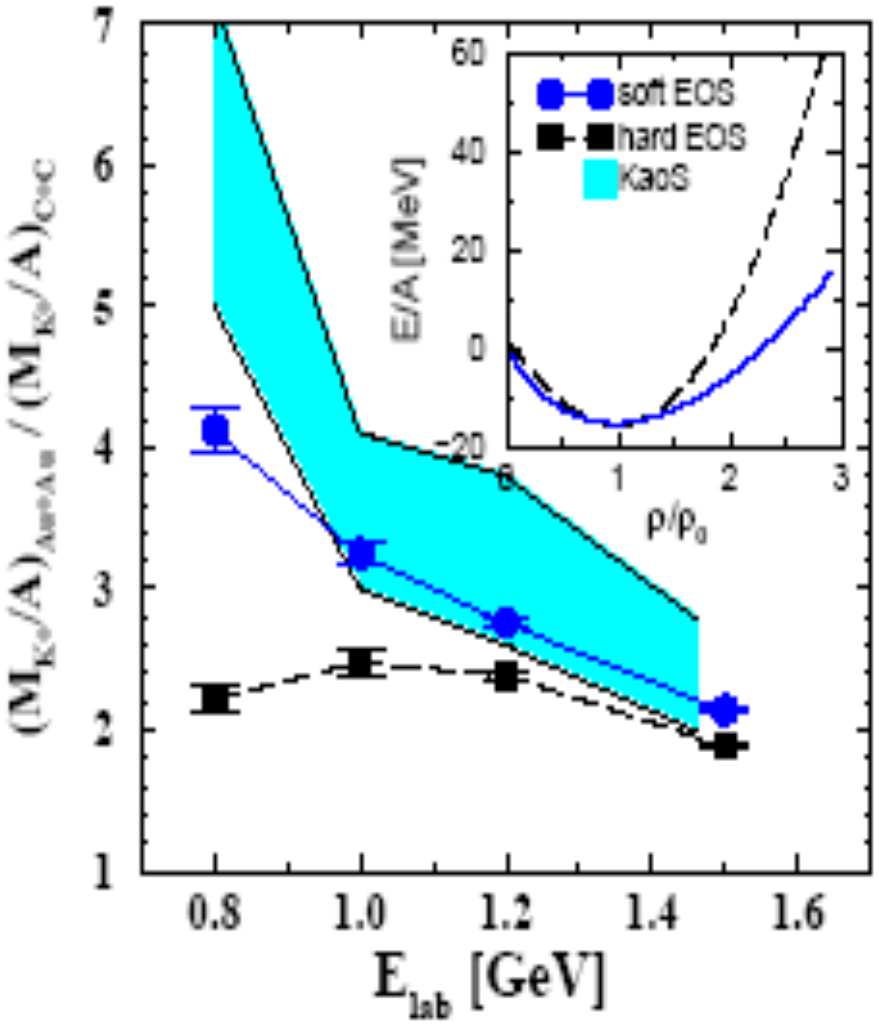

- Kaon production at subthreshold energy in HI collisions is sensitive to nuclear EOS and data are consistent with a soft one.

Theoretical predictions on nuclear symmetry energy

Zhang & Li, EJPA 55, 39 (2019)

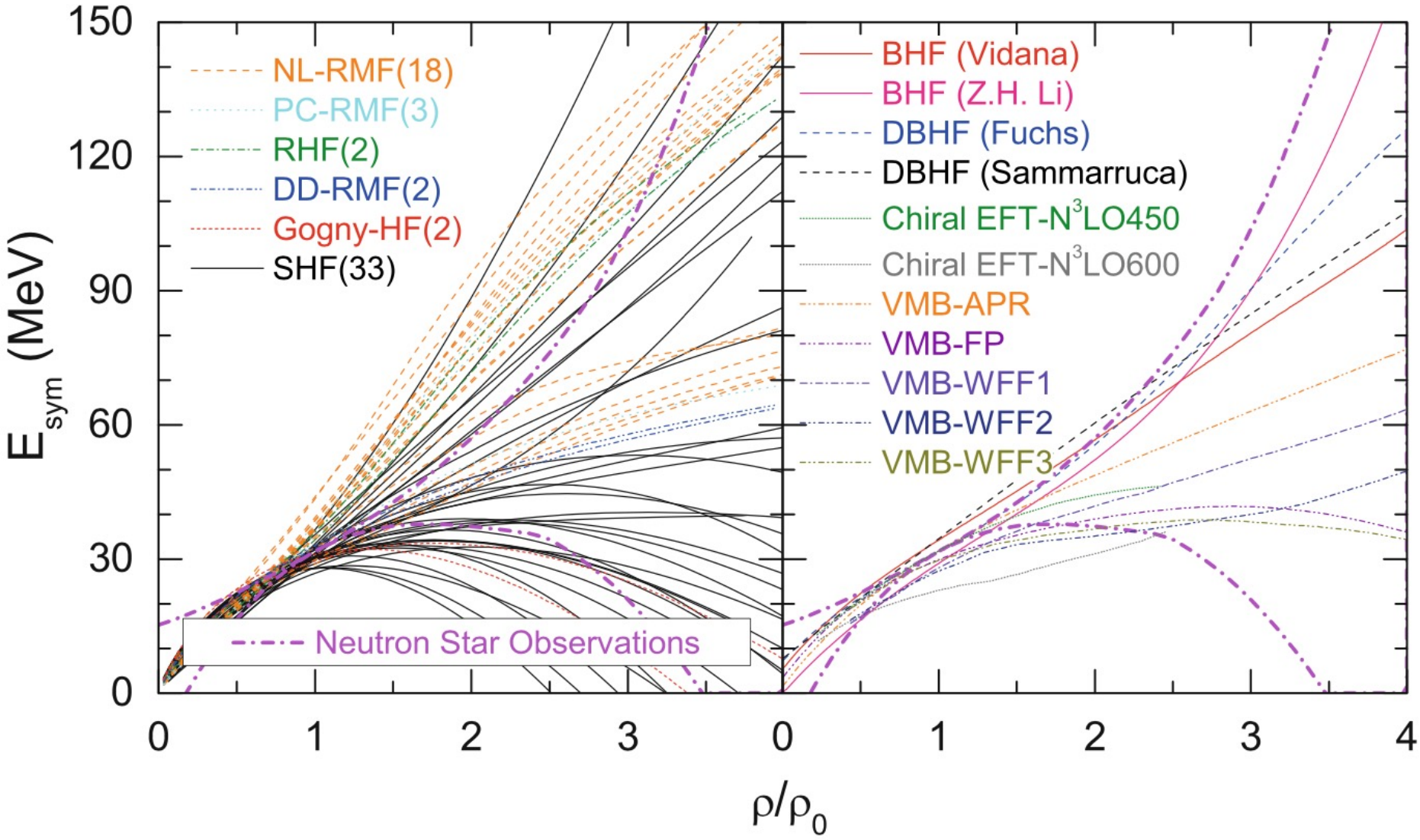

- Large uncertainties at both low and high densities

Density dependence of nuclear symmetry energy

W. G. Lynch and M. B Tsang, PLB 830, 137098 (2022)

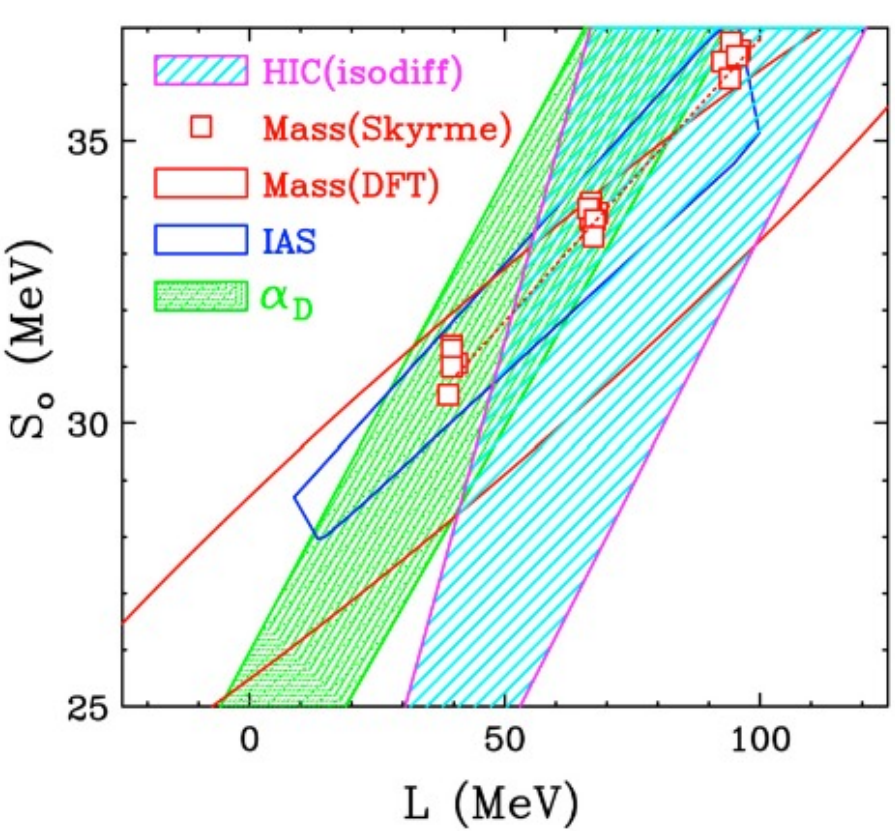

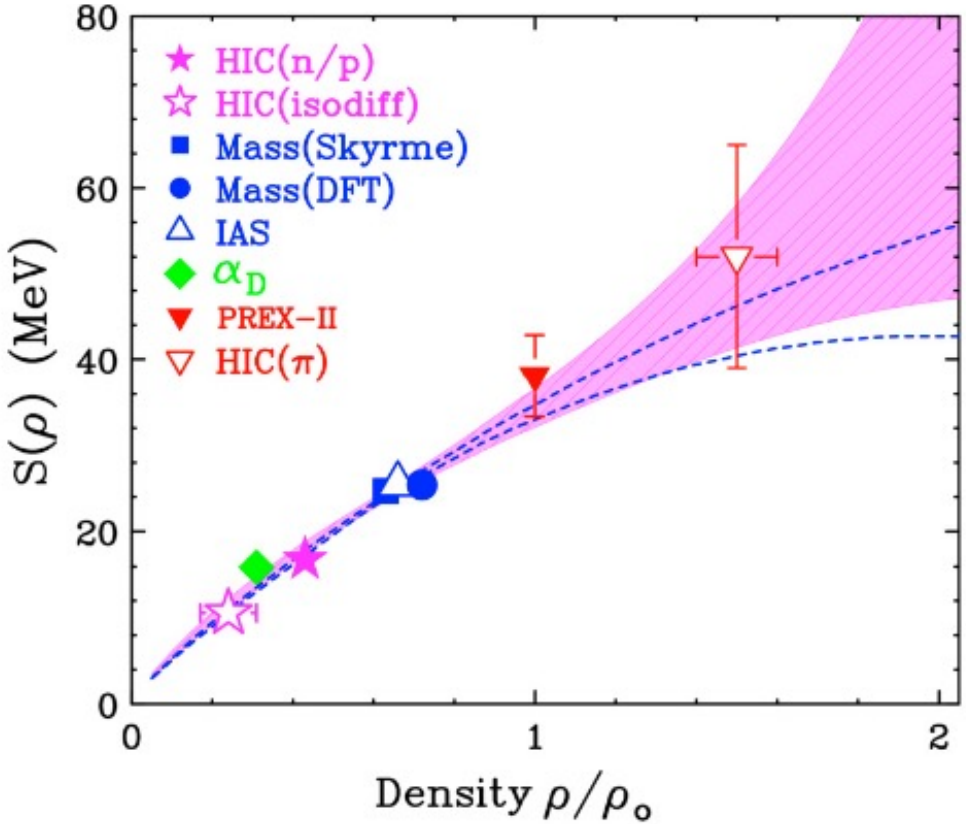

- Instead of constraining the symmetry energy S_0 and and its slope parameter L at nuclear matter saturation density (left figure), each measured observable should be used to determine the symmetry energy at the density it is most sensitive (right figure).

Hadronic potentials in nuclear medium

Ko & Li, JPG 22, 1673 (1996);
Ko, Koch & Li, ARNPS 47, 505 (1997)

- **Kaons and antikaons:** Chiral effective Lagrangian → repulsive potential for kaons and attractive potential for antikaons

$$U_{K,\bar{K}} = \omega_{K,\bar{K}} - \omega_0, \quad \omega_0 = \sqrt{m_K^2 + p^2}$$

$$\omega_{K,\bar{K}} = \sqrt{m_K^2 + p^2 - a_{K,\bar{K}}\rho_s + \left(b_K \rho_B\right)^2} \pm b_K \rho_B$$

$$a_K = 0.22\ \text{GeV}^2\text{fm}^3, \quad a_{\bar{K}} = 0.45\ \text{GeV}^2\text{fm}^3$$

$$b_K = 0.33\ \text{GeV}^2\text{fm}^3$$

$$\Rightarrow \quad U_K = 20\ \text{MeV}, U_{\bar{K}} = -120\ \text{MeV at } \rho_0 = 0.16\ \text{fm}^{-3}$$

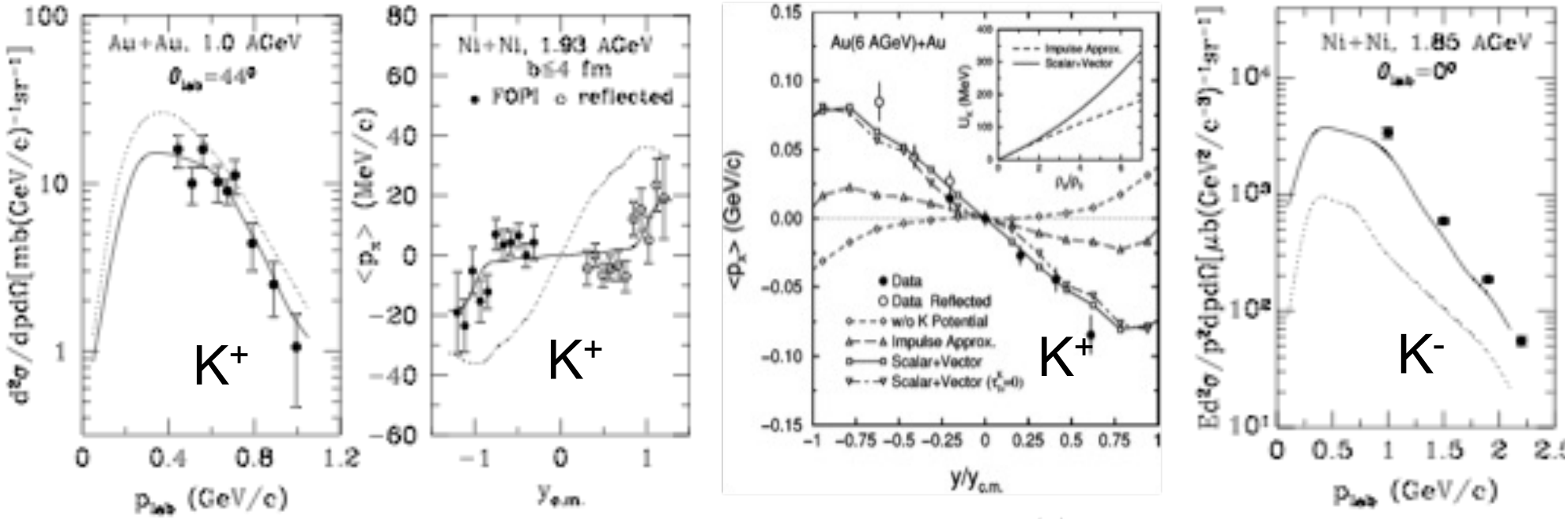

- Experimental data on spectrum and directed flow are consistent with repulsive kaon and attractive antikaon potentials.

Dilepton production from heavy ion collisions

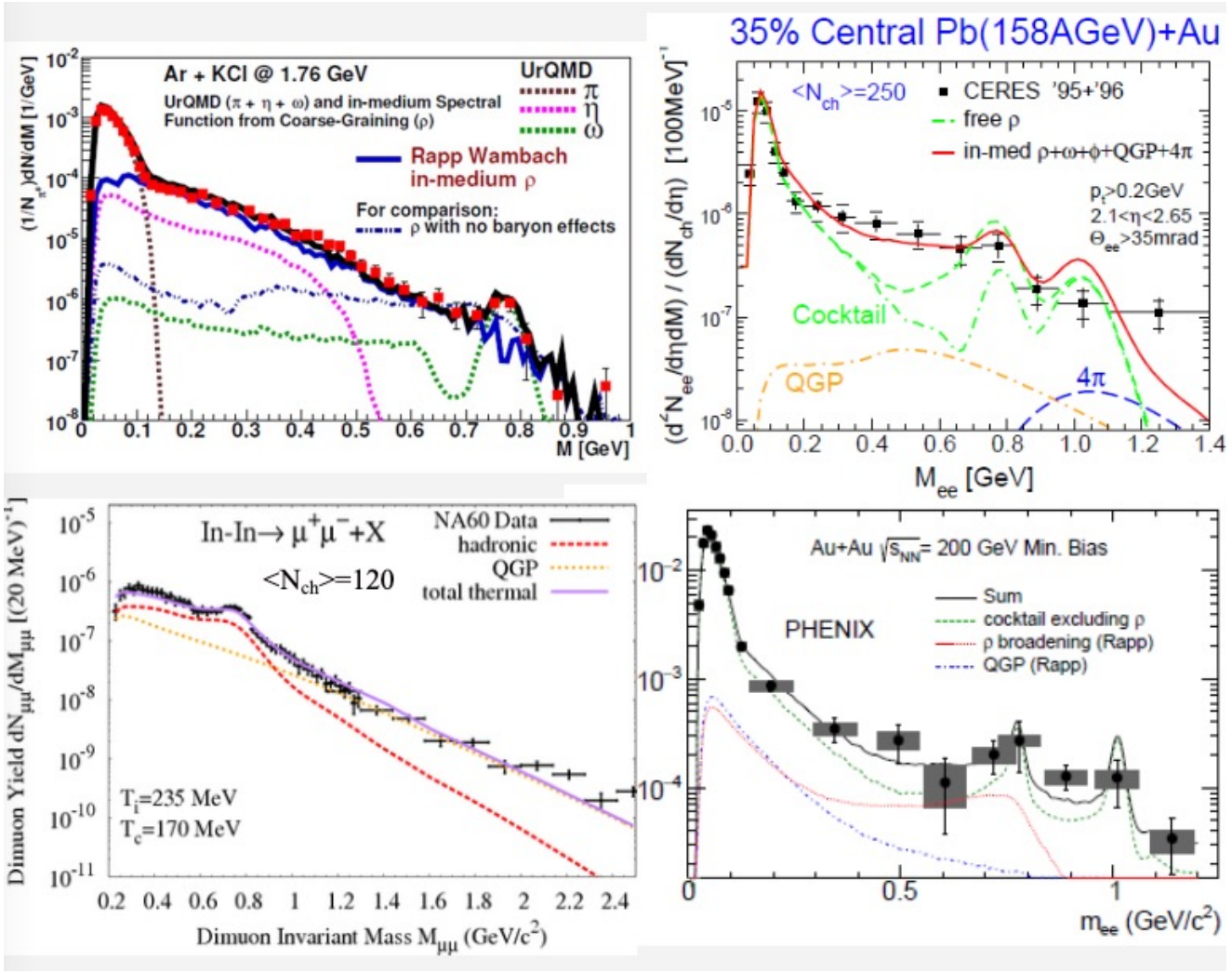

$$\frac{dR_{e^+e^-}}{d^4q} = \frac{\alpha^2}{\pi^3 M^2} f^B(q_0;T)\rho_{\rm em}(M,\mathbf{q};\mu_B,T)$$

- Melted rho meson consistent with partial restoration of chiral symmetry.

Rho meson spectral function

Given by the imaginary of in-medium rho meson propagator

$$D_\rho(M, \mathbf{q}; \mu_B, T) = [M^2 - m_\rho^2 - \Sigma_{\rho\pi\pi} - \Sigma_{\rho B} - \Sigma_{\rho M}]^{-1}$$

- In-medium pion cloud

Asakawa & Ko, Chafray et al,
Urban et al, Weise et al, Koch et al.

$\Sigma_{\rho\pi\pi}$ =

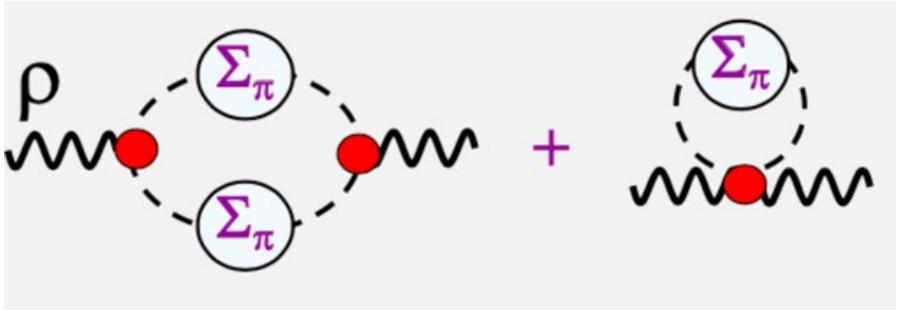

Based on the Delta-hole model for pion in-medium interactions

- Direct ρ-hadron scattering

Friman et al., Rapp et al.,
Post et al.

$\Sigma_{\rho BM}$ =

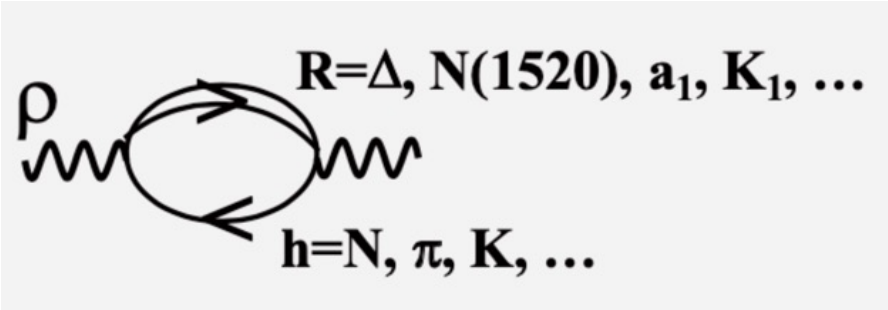

Estimate couplings from $R \to \rho N, \gamma N$
Based on scattering data from $\pi N \to \rho N, \gamma N \to, \gamma A \to, \ldots$.

Hydrodynamic model

Kolb & Heinz; Teany & Shuryak; Hirano, ……..

Hydrodynamic Equations

$$\partial_\mu T^{\mu\nu}(x) = 0$$ Energy-momentum conservation

$$\partial_\mu n_j u^\mu(x) = 0$$ Charge conservations (baryon, strangeness,…)

For viscous fluids with viscosity

$$T^{\mu\nu}(x) = [e(x) + p(x)]u^\mu(x)u^\nu(x) - p(x)g^{\mu\nu} + \pi^{\mu\nu}$$

e: energy density
p: pressure
u^μ: four velocity
$\pi^{\mu\nu}$: shear tensor

Equation is closed by the equation of state p(e) and depends on the shear viscousity η. Particlization from Cooper-Frye instaneous freeze-out

$$E\frac{dN_i}{d^3q} = \frac{g_i}{(2\pi 2^3}\int q\cdot d\sigma \frac{1}{\exp(q\cdot u)\pm 1}$$

dσ is an element of space-like hypersurface

- Applicable for relativistic heavy ion collisions in which QGP is formed.

Statistical model

Braun-Munzinger and Donigus, NPA 987, 144 (2019)

Assume thermally and chemically equilibrated system of non-interacting hadrons and resonances with density

$$n_i = \frac{g}{2\pi^2}\int_0^\infty \frac{p^2 dp}{e^{(E_i(p)-\mu_i)/T} \pm 1}, \quad E_i = \sqrt{p^2 + m_i^2}$$

Determine chemical freeze out temperature T_{ch} and baryon chemical potential μ_B by fitting experimental data after inclusion of feed-down from short lived particles and resonances decay.

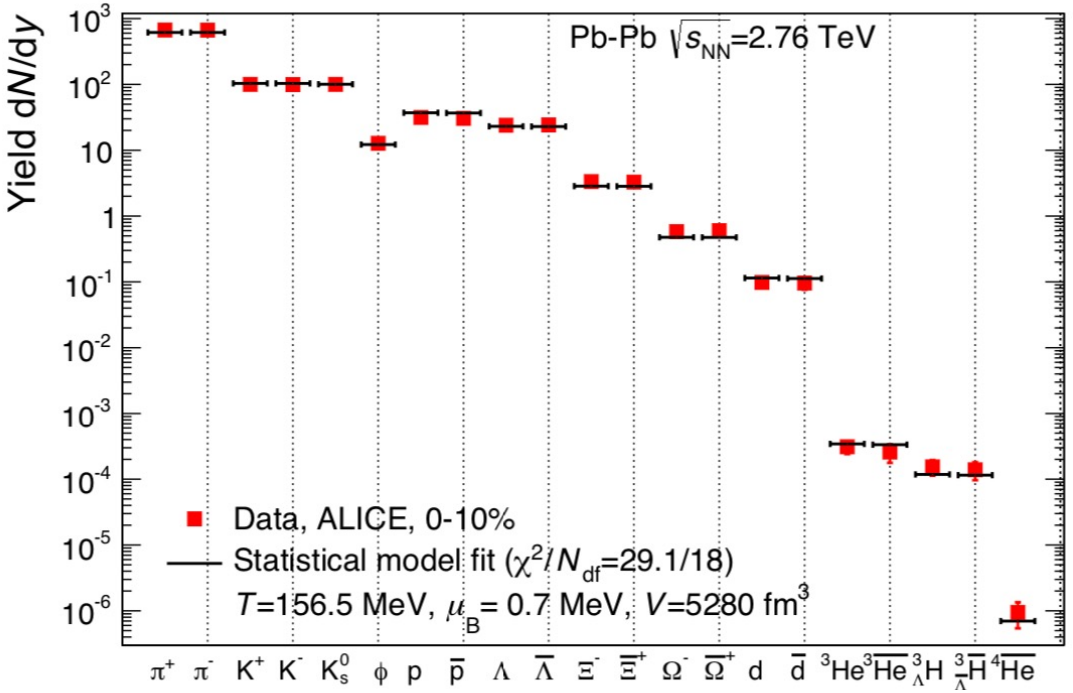

$T_{ch} \sim T_c$

Transverse momentum spectra from hydrodynamic model

Kolb & Heinz, nucl-th/0305084

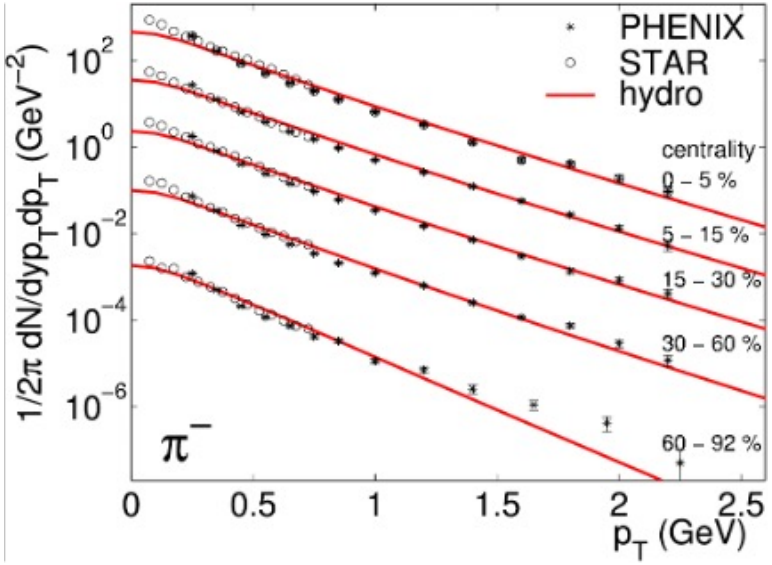

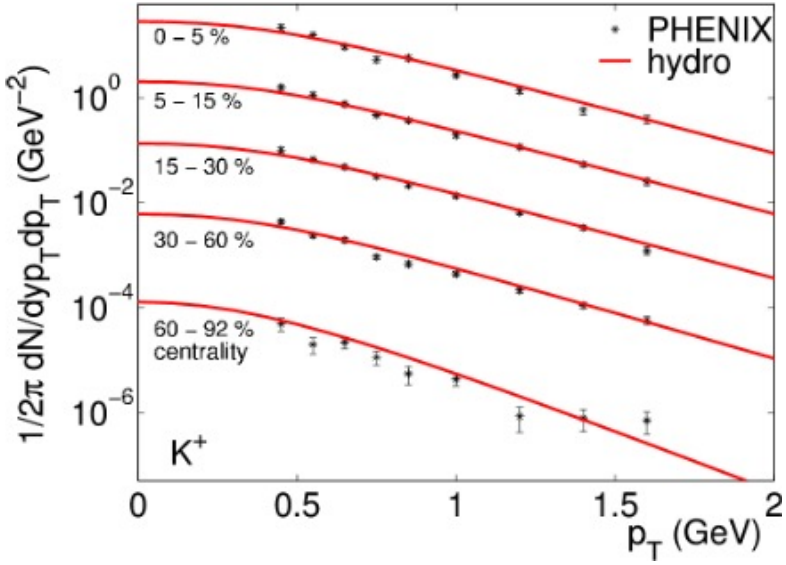

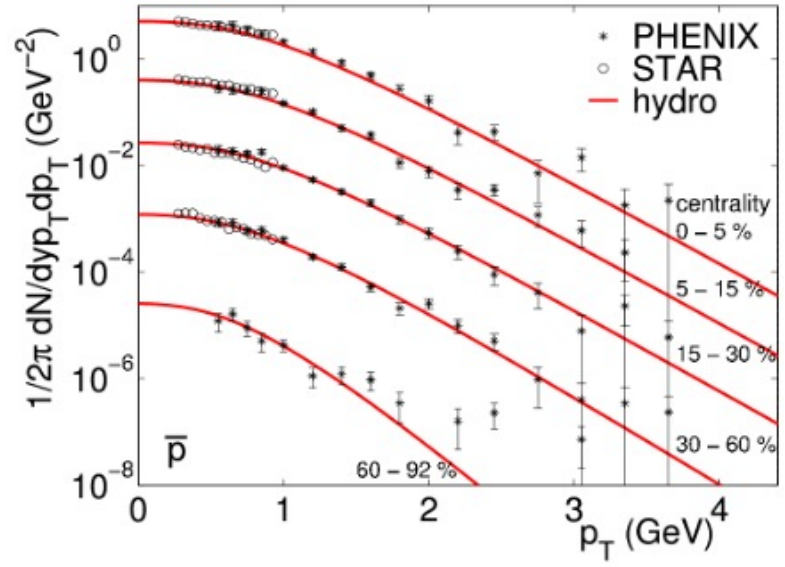

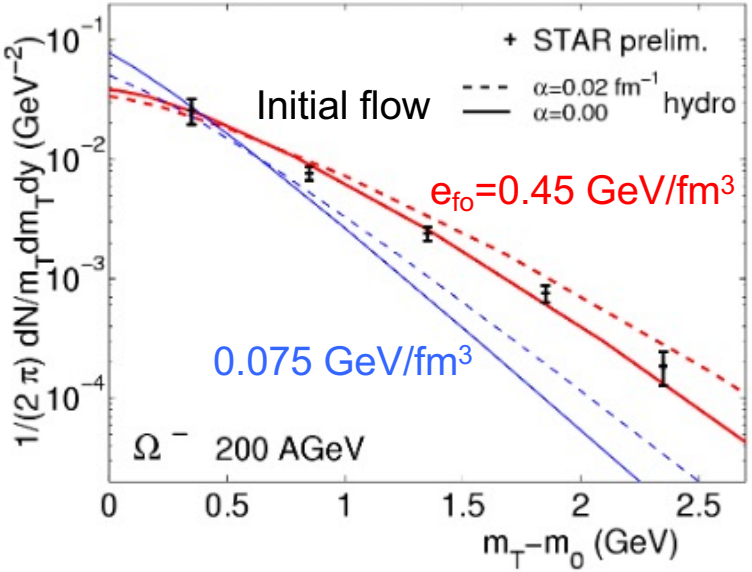

Initial T_i=340 MeV, e_i=25 GeV/fm^3

Freezeout T_f=128 MeV

Elliptic flow from hydrodynamic model

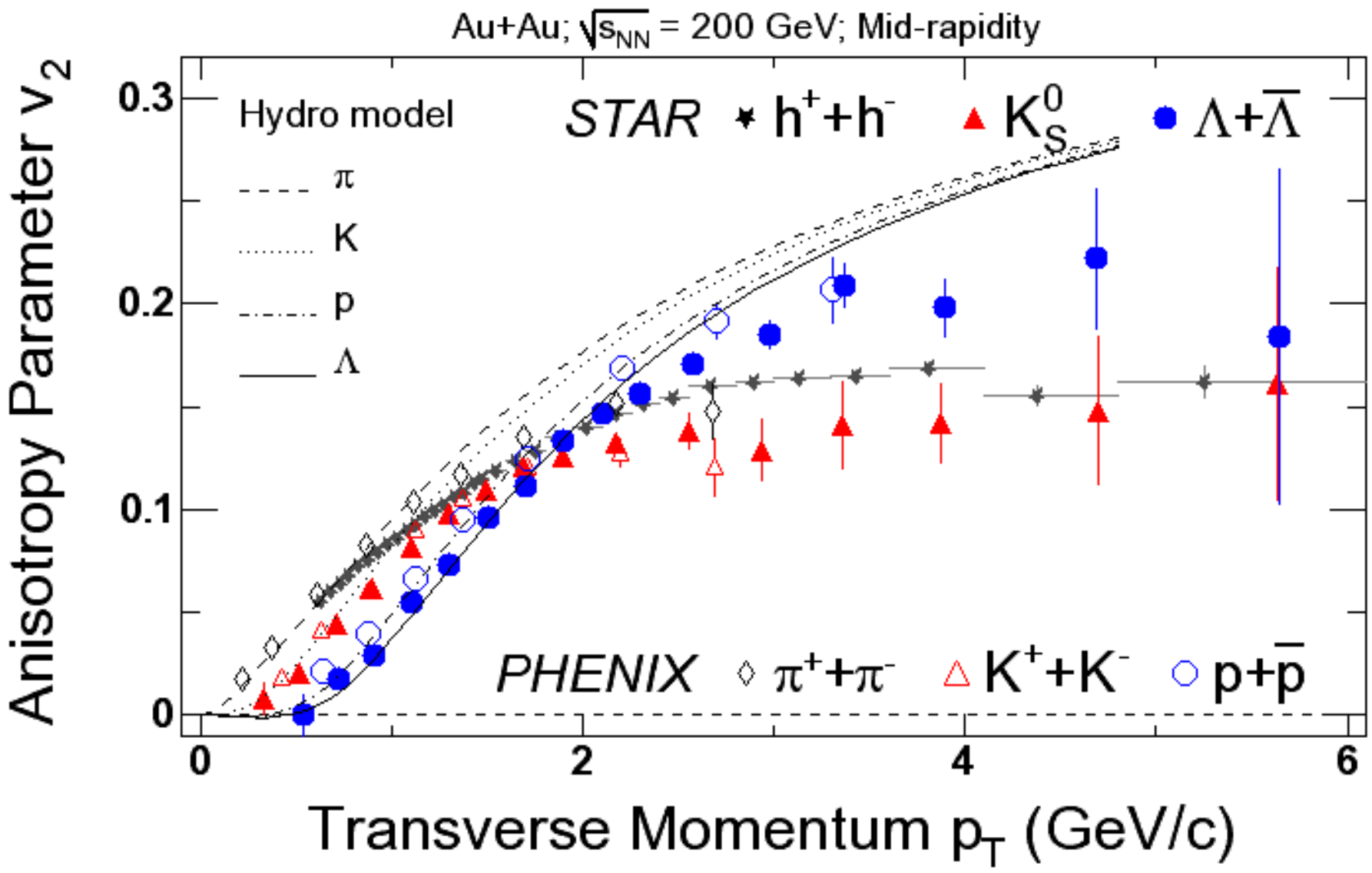

- Ideal hydro describes very well data at low p_T (mass effect) but fails at intermediate p_T → viscous or nonequlibrium effect

Viscous effects on elliptic flow

Romatschke & Romatschke, PRL 99, 172301 (2007)

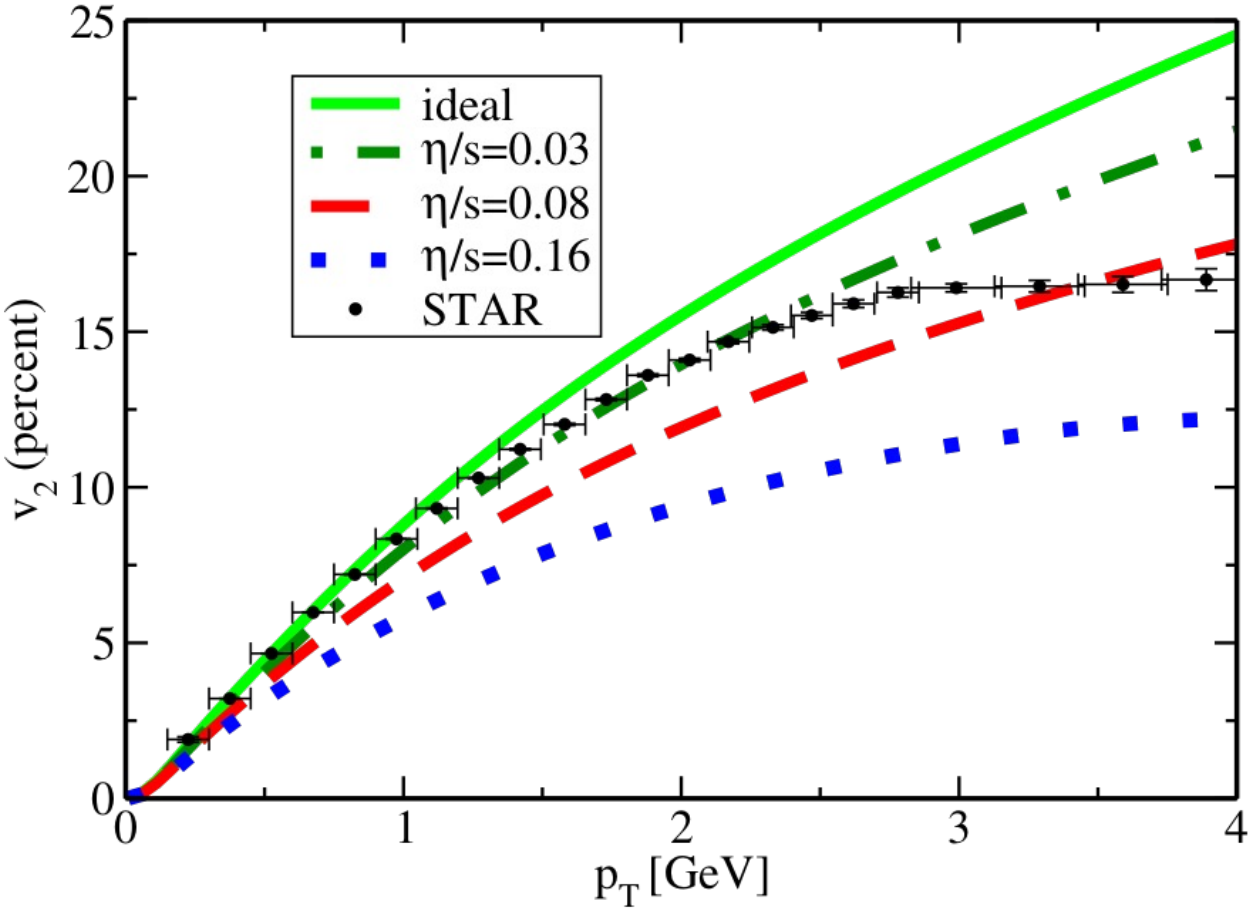

- Data requires small viscosity to entropy density ratio $0.03 \leq \eta/s \leq 0.08$

Elliptic flow from AMPT

Lin & Ko, PRC 65, 034904 (2002)

AMPT: A multiphase transport model that includes both partonic and Hadronic scattering; Lin, Pal, Zhang, Li & Ko, PRC 61, 067901 (00); 64, 041901 (01); 72, 064901 (05); https://myweb.ecu.edu/linz/ampt/

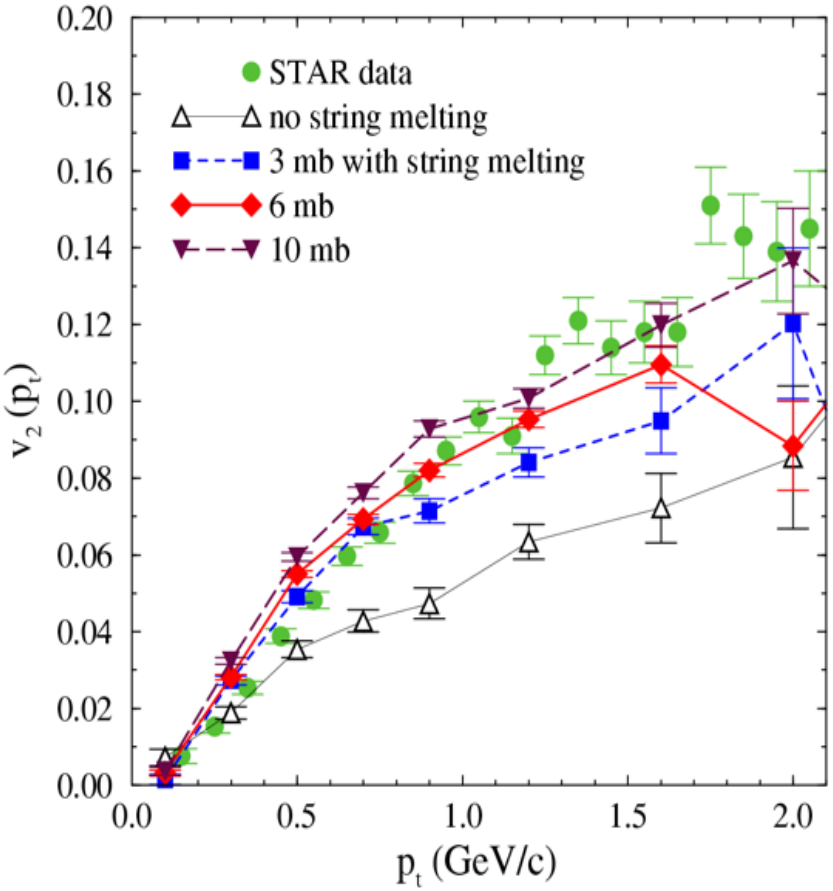

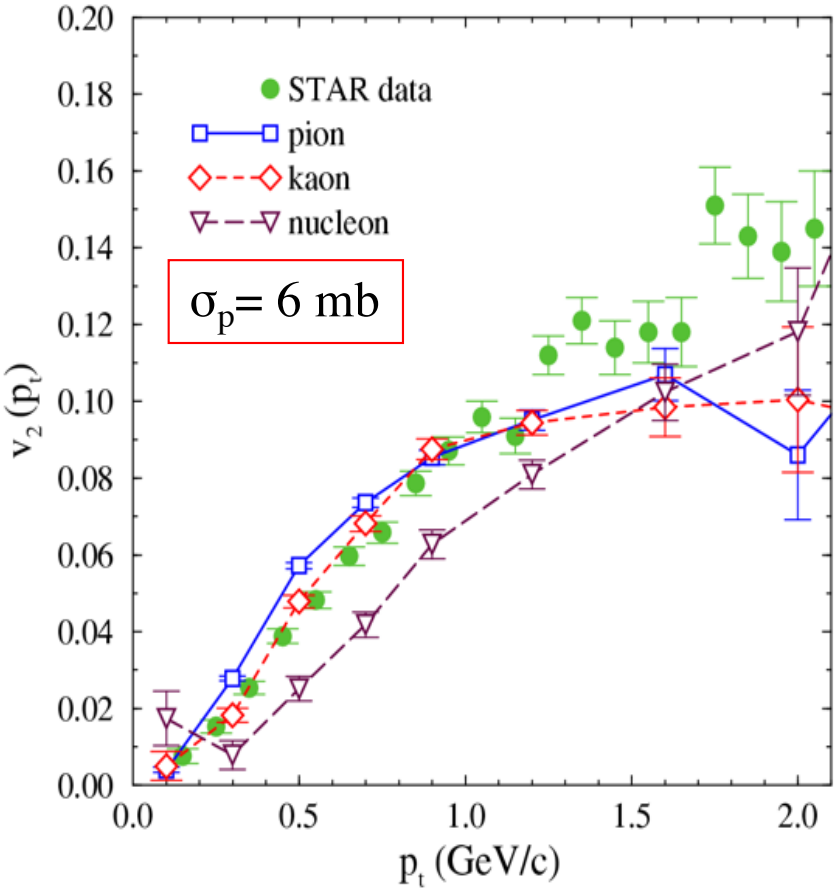

- Need string melting and large parton scattering cross section
- Mass ordering of v_2 at low p_T as in hydrodynamic model

Valence quark number scaling of hadron elliptic flow

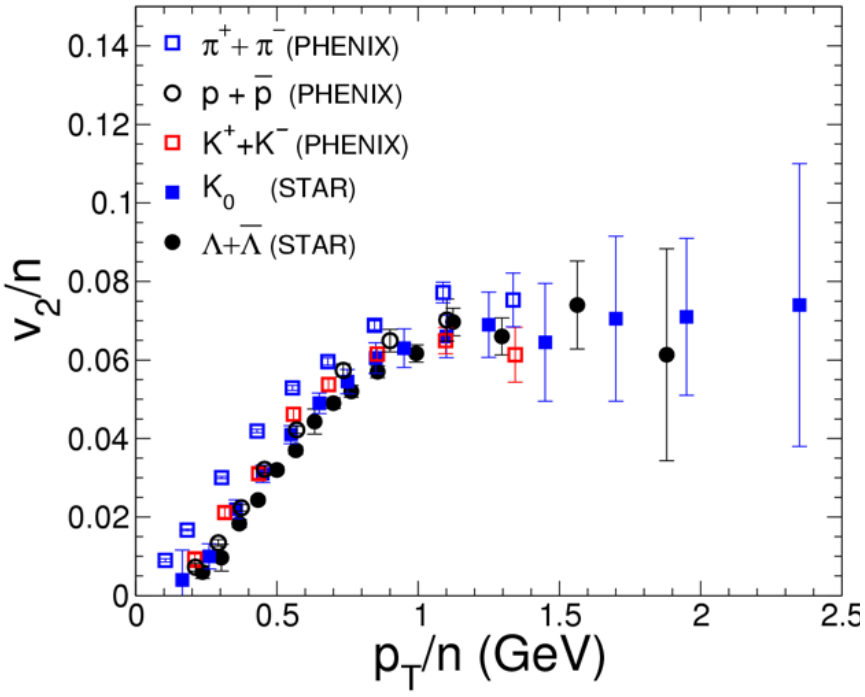

Kolb, Chen, Greco & Ko, PRC 69, 051901 (04)

Naïve quark coalescence model:
Only quarks of same momentum can coalesce or recombine.

- Quark transverse momentum distribution

$$f_q(p_T) \propto 1 + 2v_{2,q}(p_T)\cos(2\varphi)$$

- Meson elliptic flow

$$v_{2,M}(p_T) = \frac{2v_{2,q}(p_T/2)}{1+2v_{2,q}^2(p_T/2)} \approx 2v_{2,q}(p_T/2)$$

- Baryon elliptic flow

$$v_{2,B}(p_T) = \frac{3v_{2,q}(p_T/3)}{1+6v_{2,q}^2(p_T/3)} \approx 3v_{2,q}(p_T/3)$$

Quark number scaling:

$$\frac{1}{n} v_2(p_T/n)$$

same for mesons and baryons except pions which are mainly from resonance decays (Greco & Ko, PRC 70, 024901 (04))

Large proton to pion ratio

Quark coalescence or recombination can also explain observed large p/pi ratio at intermediate transverse momentum in central Au+Au collisions.

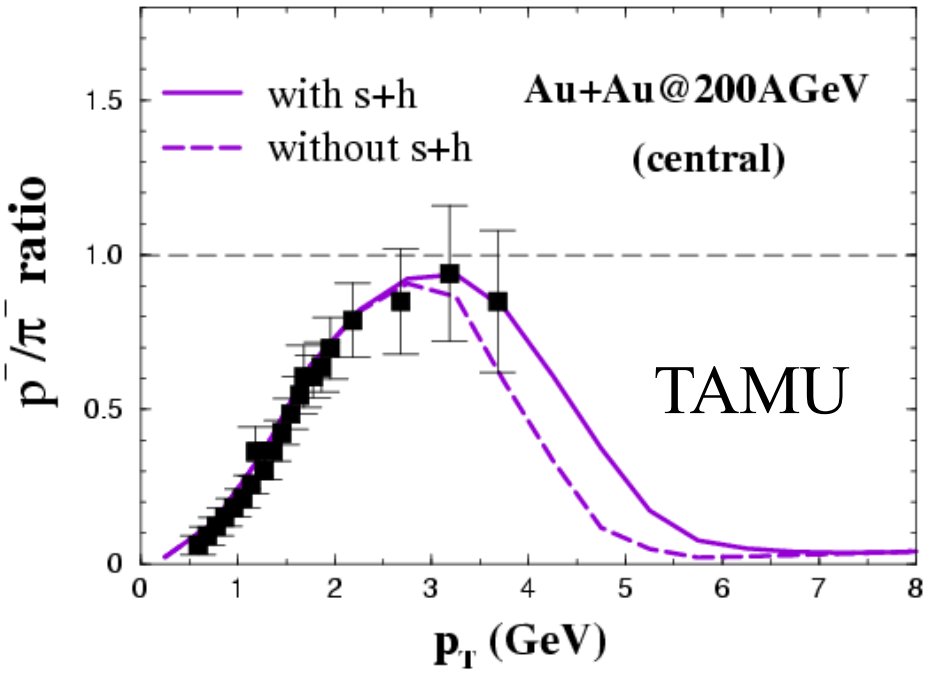

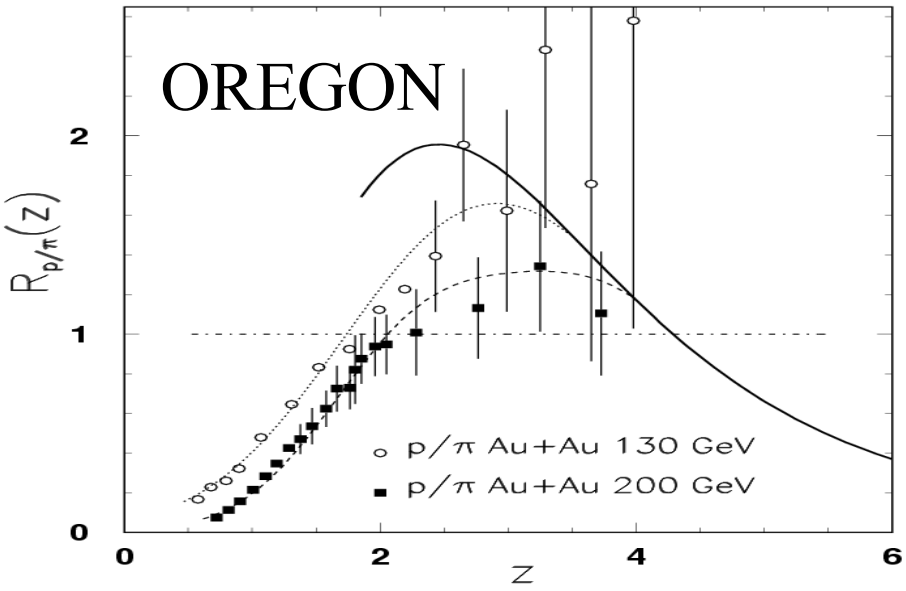

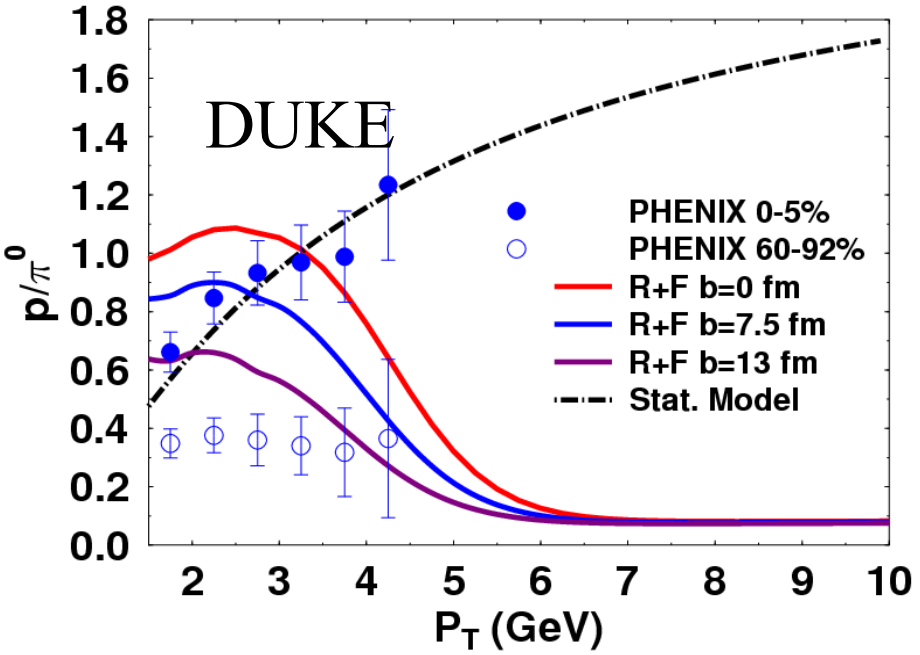

Λ_c to D0 ratio in experiments and models

Plumari et al., EPJC 78, 348 (2018)

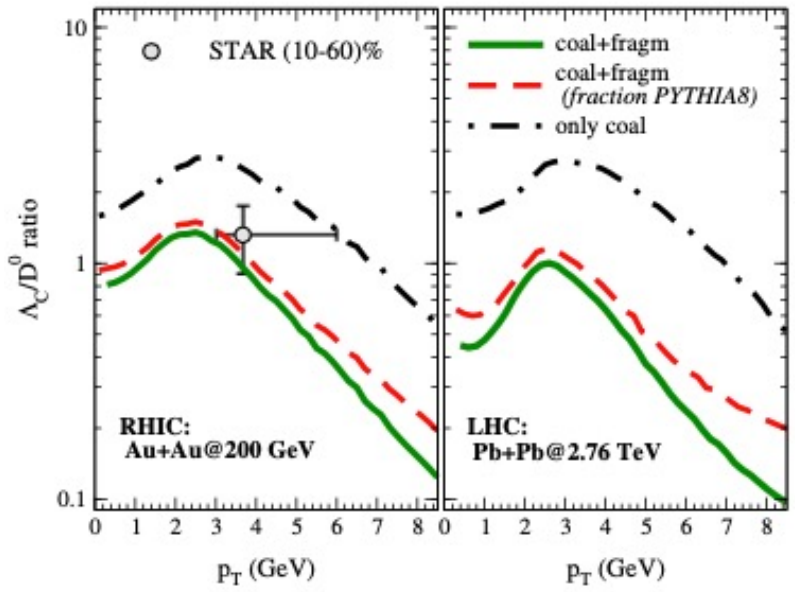

Cao et al., PLB 807, 135561 (2020);
Cho et al., PRC 101, 024909 (2020)

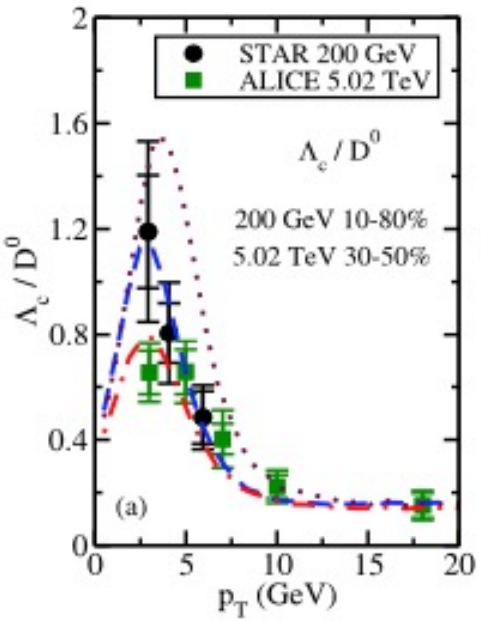

He & Rapp, PRL 124, 042301 (2020)

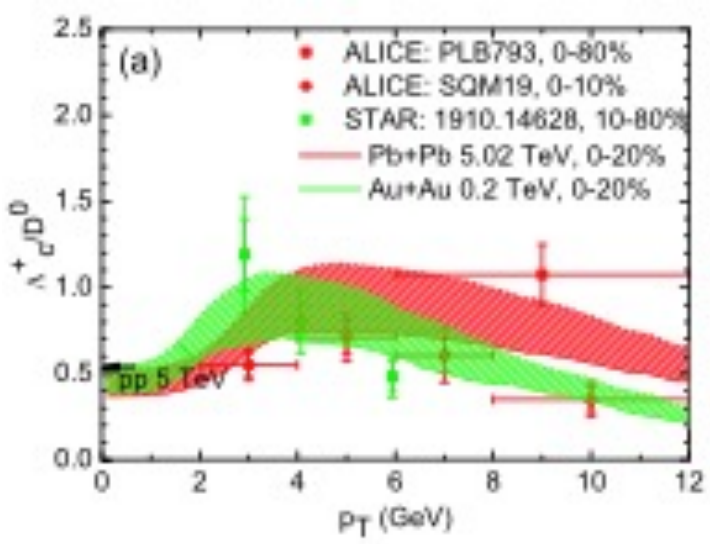

Coalescence model with contribution of known resonances and renormalized coalescence probability of unity for zero momentum charm quarks.

Coalescence model with contribution from known resonances and including the flow effect.

Energy conserving coalescence model with contributions from known and also missing resonances.

High P_T hadron suppression

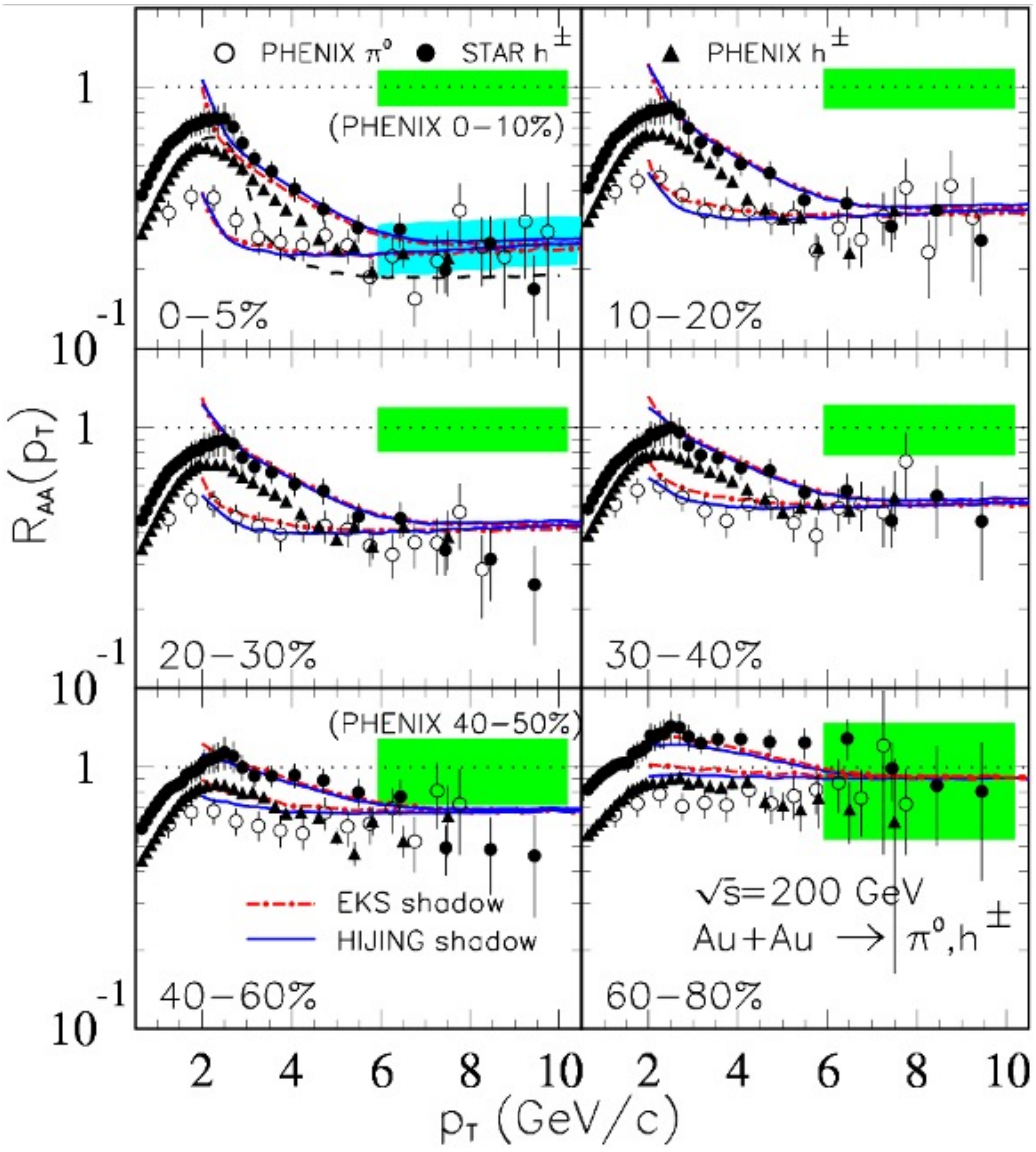

$$R_{AA} = \frac{dN_{Au+Au}}{\langle T_{AA} \rangle d\sigma_{p+p}}$$

Gyulassy, Levai & Vitev, PRL 85, 5535 (00)

Wang & Wang, PRL 87, 142301 (01)

Parton energy loss due to radiation

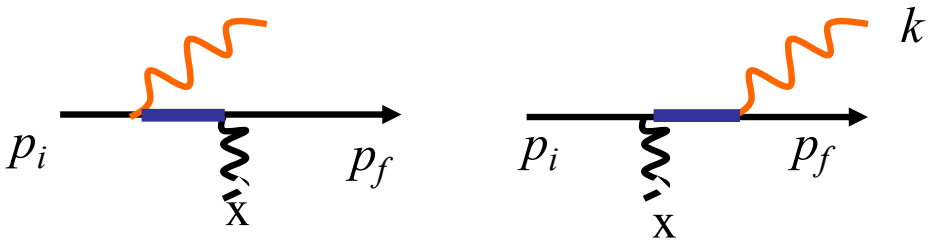

$$\frac{dE}{dx} = -C_2 \alpha_s \hat{q} L$$

- Jet quenching $\rightarrow \hat{q} = 0.8 - 1.7$ GeV^2/fm

J/ψ absoprtion and production in HIC

- Nuclear absorption: $J/\psi + N \rightarrow D + \Lambda_c$; p+A data $\rightarrow \sigma \sim 6$ mb
- Absorption and regeneration in QGP: $J/\Psi + g \leftrightarrow c\bar{c}$
- Absorption and regeneration in hadronic matter: $J/\Psi + \pi \leftrightarrow D\bar{D}$

Zhao & Rapp, arXiv:0810.4566 [nucl-th]

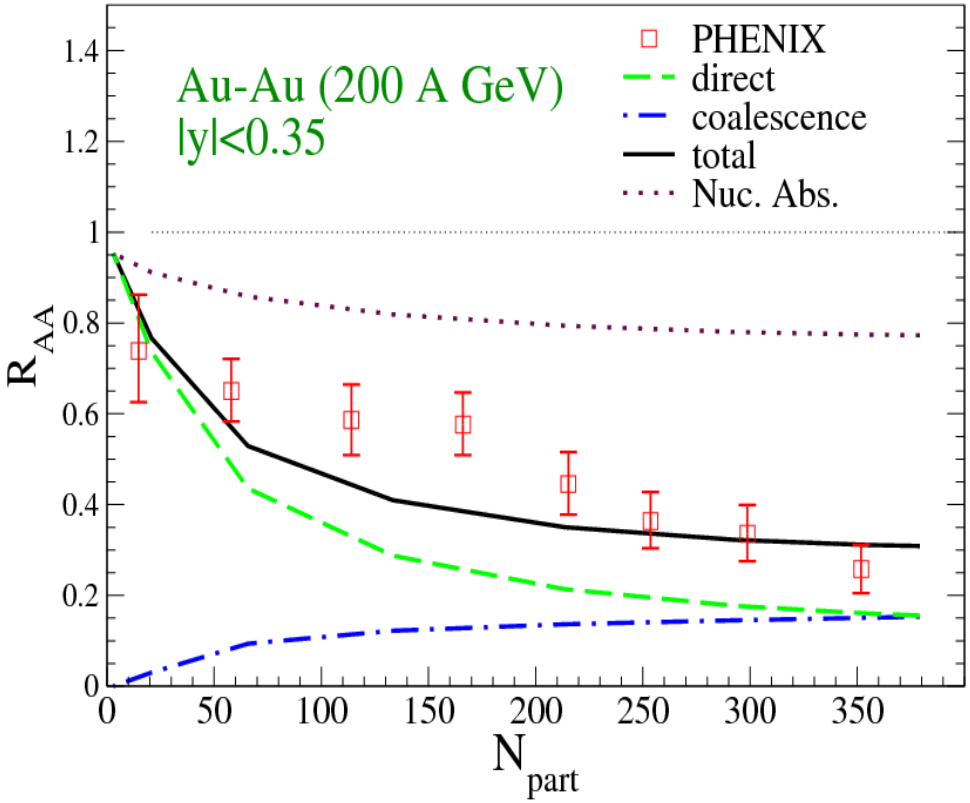

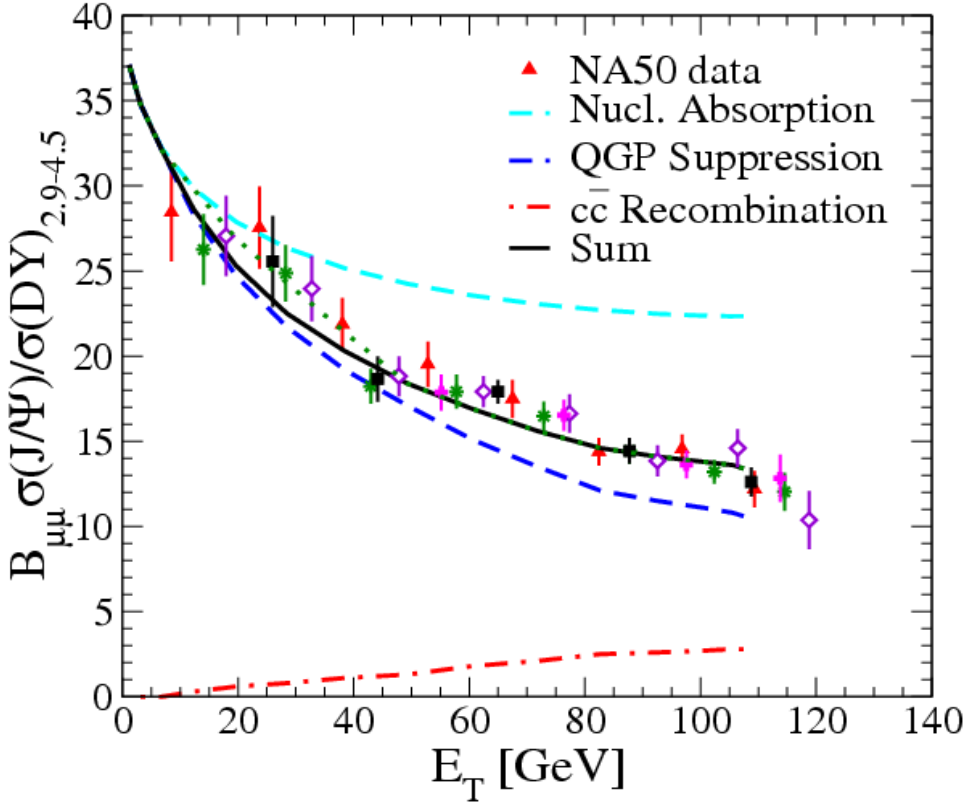

- Suppressed production at large N_{part} $\rightarrow$ melting of J/Ψ due to color screening.
- Regeneration from coalescence of charm and anticharm quark is non-negligible at RHIC.

Heavy flavor quenching and flow

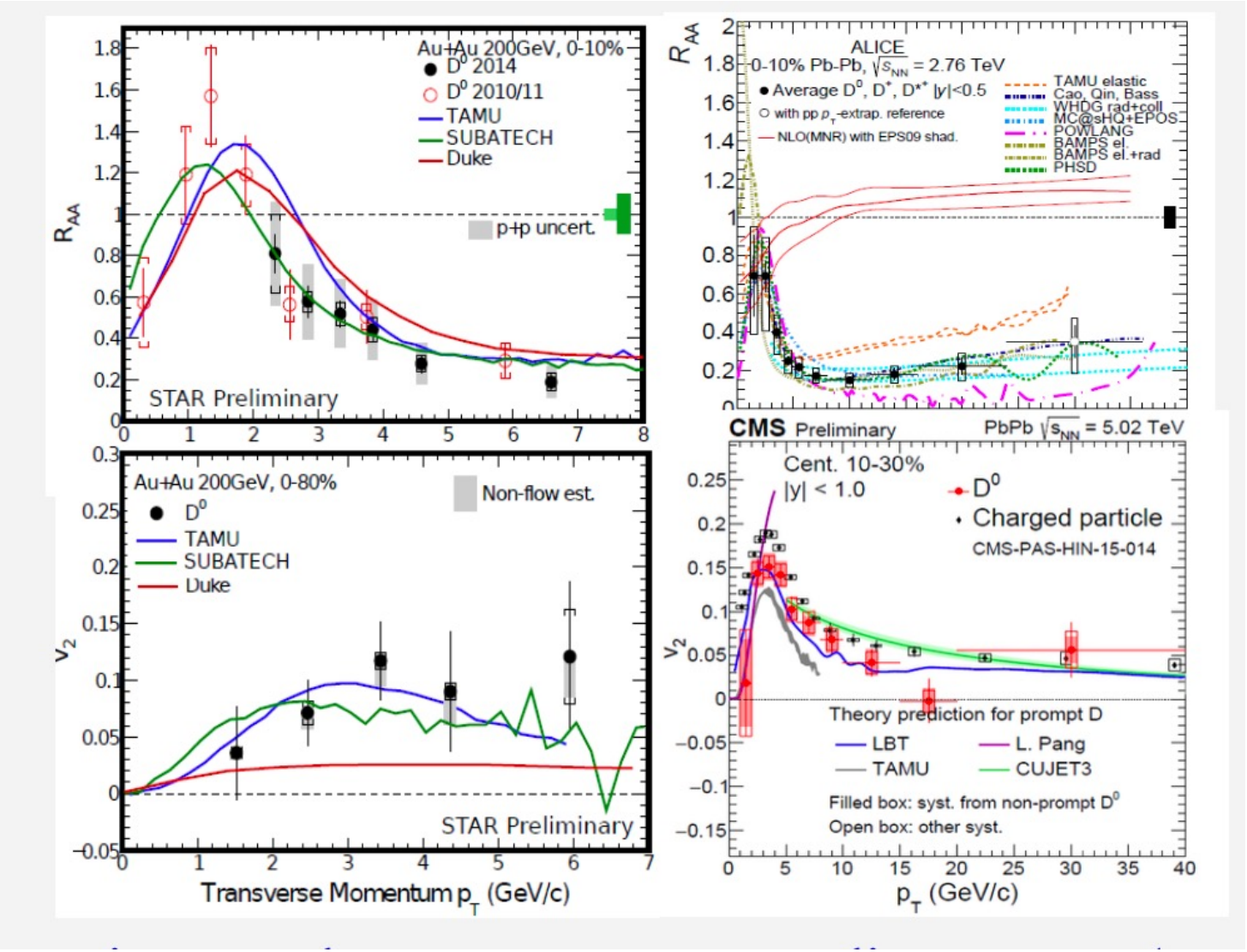

$$\frac{\partial f}{\partial t} = \gamma \frac{\partial (pf)}{\partial p} + D_p \frac{\partial^2 f}{\partial p^2}$$

- Small diffusion coefficient D_p or large drag coefficient γ

Yield ratio of $N_t N_p / N_d^2$ in Au+Au collisions at RHIC

STAR Collaboration, PRL 130, 202301 (2023)

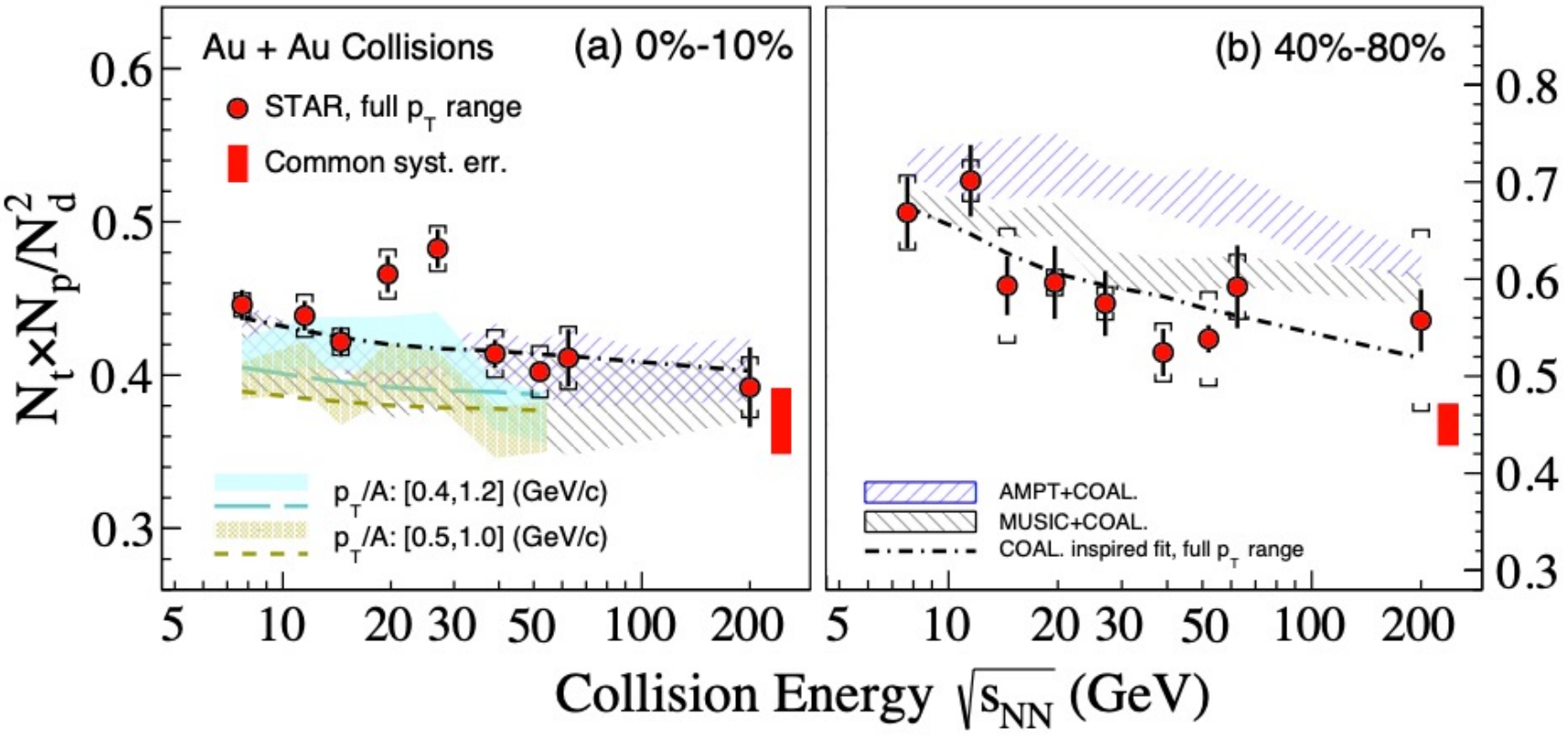

- Enhanced yield ratio of $N_t N_p / N_d^2$ at $\sqrt{s_{NN}} \approx 25$ GeV in central Au+Au collisions, compared to non-central collisions.
- Possible signature of a first-order phase transition → density fluctuation → $\frac{N_t N_p}{N_d^2} \approx g(1 + \Delta\rho_n)$, where $\Delta\rho_n$ = neutron density fluctuation.

Transport description of quark matter in a box based on NJL

$$\partial_t f + \mathbf{p}/E \cdot \nabla f - \nabla H \cdot \nabla_p f = \mathcal{C}[f]$$ Feng & Ko, PRC 93, 035205 (16); 95, 055203 (17)

C[f] includes quark elastic scattering with cross section of 3 mb

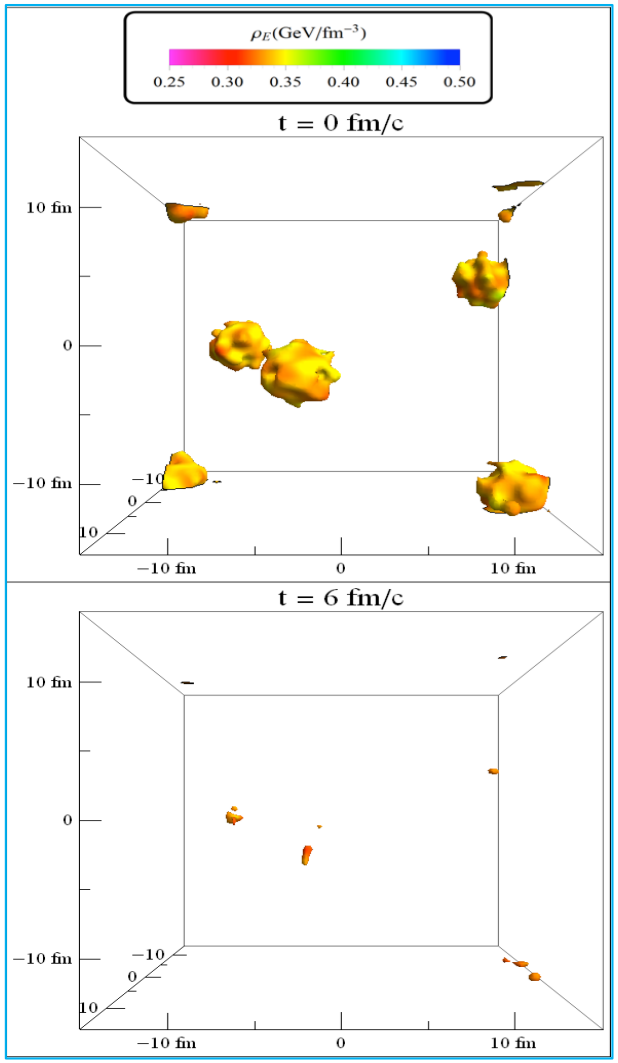

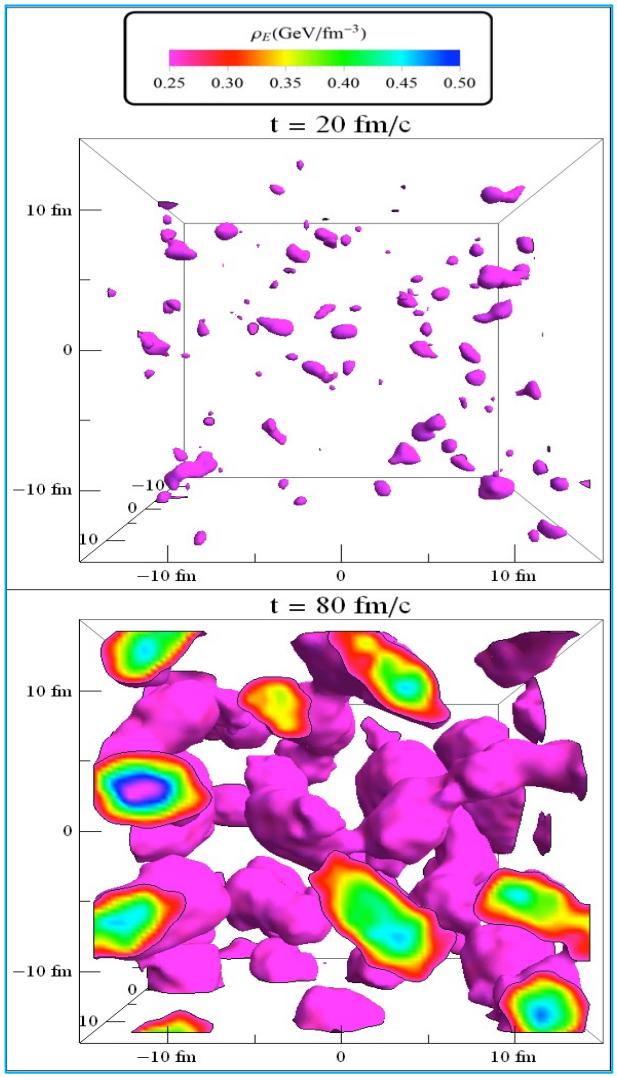

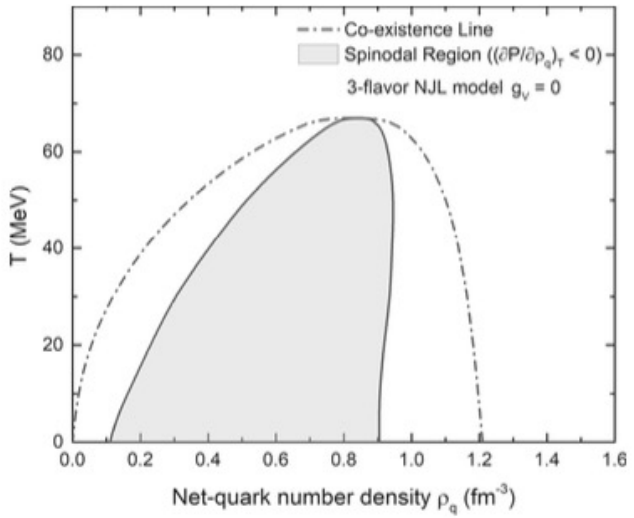

- Left: $n_q = 0.4/fm^3$, T = 100 MeV; outside spinodal region
- Right: $n_q = 0.4/fm^3$, T = 20 MeV, inside spinodal region; large density fluctuations appear due to growth of unstable modes
- Colored regions correspond to $n_q > 0.6/fm^3$

Light nuclei production from non-local many-body scattering

Sun, Wang, Ko, Ma & Shen, Nature Communications 15, 1074 (2024)

$$\frac{\partial f_d}{\partial t}+\frac{\mathbf{P}}{E_d}\cdot\frac{\partial f_d}{\partial \mathbf{R}}=\frac{1}{2g_dE_d}\int\prod_{i=1}^{3}\frac{\mathrm{d}^3\mathbf{p}_i}{(2\pi)^3 2E_i}\frac{\mathrm{d}^3\mathbf{p}_\pi}{(2\pi)^3 2E_\pi}\frac{E_d\mathrm{d}^3\mathbf{r}}{m_d}2m_dW_d(\tilde{\mathbf{r}},\tilde{\mathbf{p}})$$

$$\left(\overline{|\mathcal{M}_{\pi^+n\to\pi^+n}|^2}+n\leftrightarrow p\right)\left[-g_\pi f_\pi g_d f_d\prod_i^3(1\pm f_i)+\frac{3}{4}(1+f_\pi)(1+f_d)\prod_{i=1}^{3}g_i f_i\right]$$

$$\times(2\pi)^4\delta^4(p_1+p_2+p_3-p_\pi-p_d)\rightarrow \text{Good description of data}$$

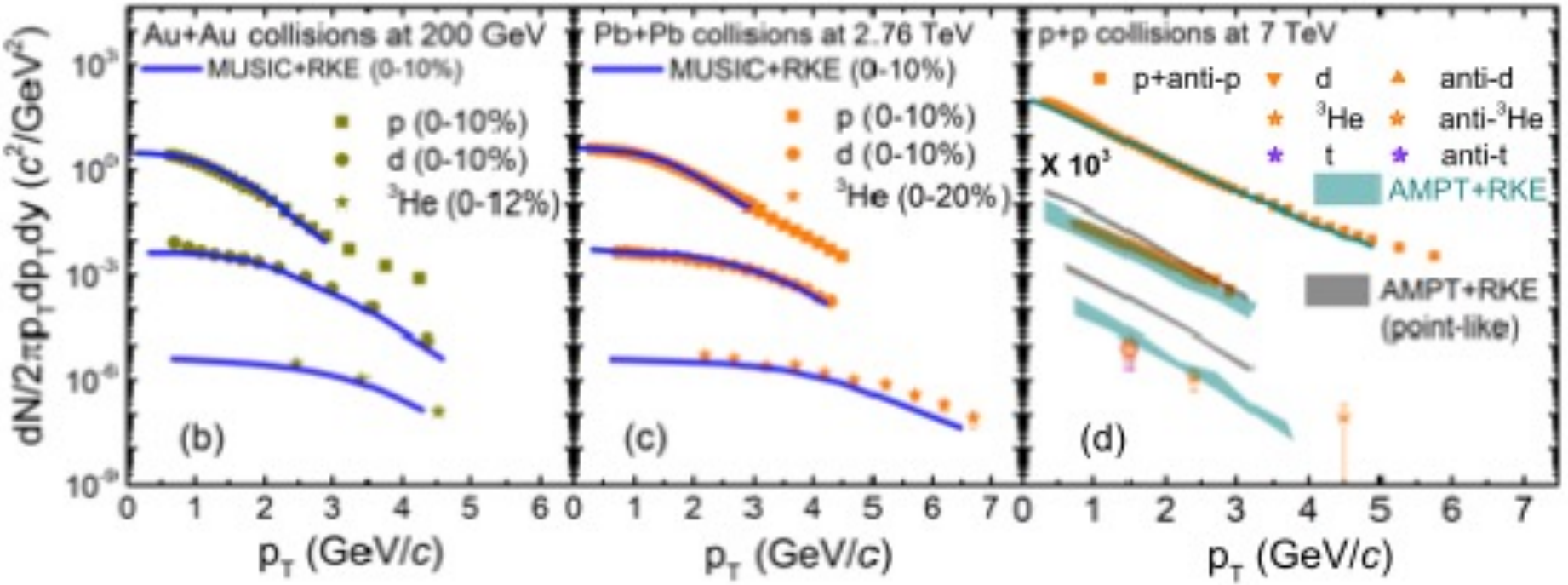

Electromagnetic field in relativistic HIC

W. T. Deng and X. G. Huang, PRC 85, 044907 (2012)

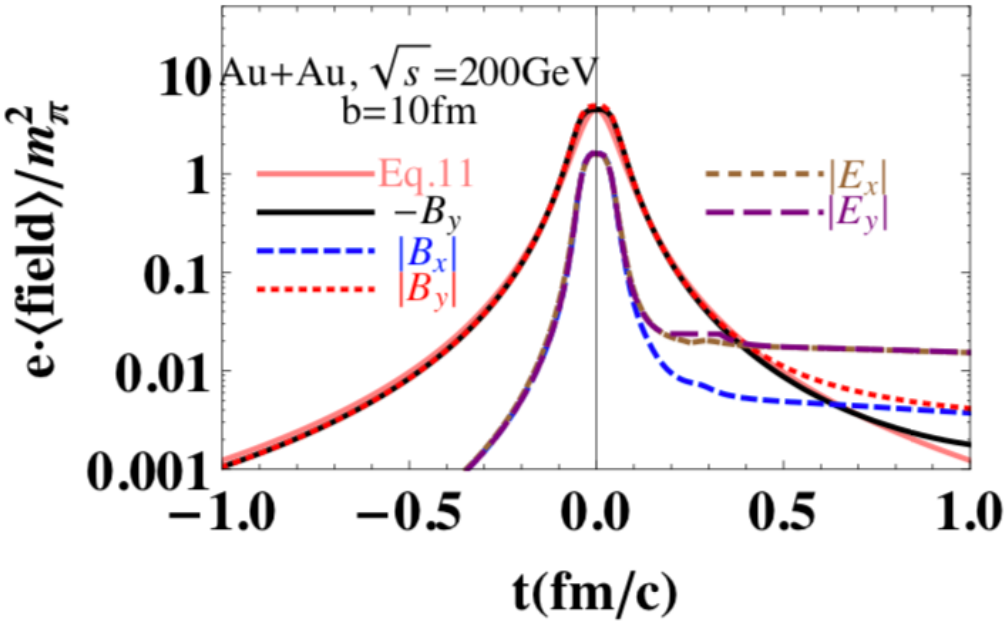

$$\langle eB_y(t)\rangle \approx \frac{\langle eB_y(0)\rangle}{(1+t^2/t_B^2)^{3/2}}$$

$$t_B \approx \frac{R_A}{\gamma v_z} \approx \frac{2m_N}{\sqrt{s}} R_A \approx 0.065 \text{ fm}$$

Calculated from the Lienard-Wiechert potential using the spatial and momentum information of the protons from HIJING.

Mclerran & Skokov, NPA 929, 184 (2014)

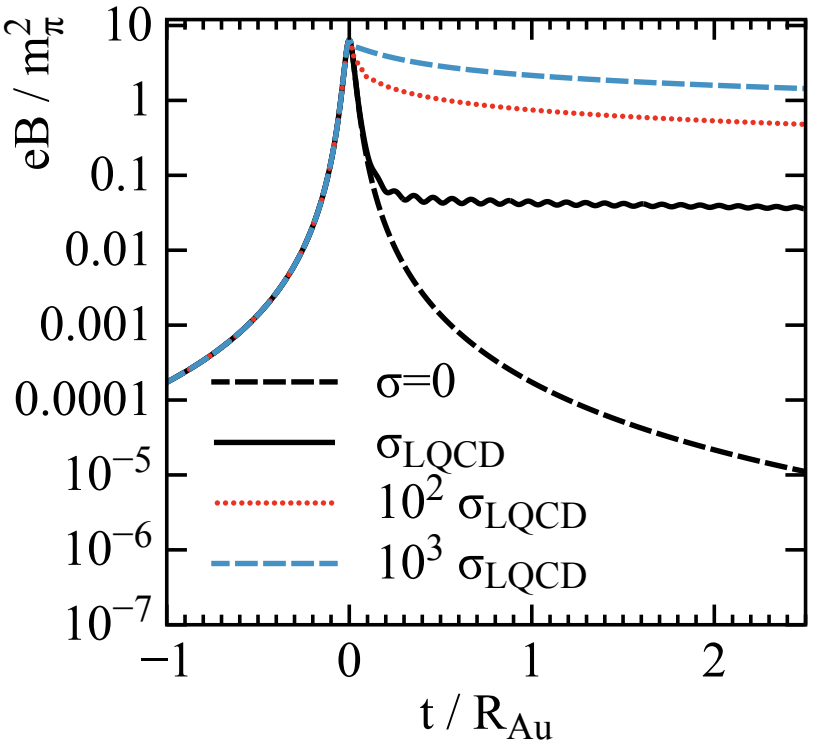

$$\sigma_{\text{Ohm}}^{\text{LQCD}} = (5.8 \pm 2.9)\frac{T}{T_0} \text{ MeV}$$

Lifetime of magnetic field is long only if QGP is a perfect conductor, which is not supported by LQCD.

Vorticity in relativistic heavy ion collisions

Jiang, Lin & Liao, PRC 94, 044910 (2016)

$$\boldsymbol{\omega} = \frac{1}{2}\boldsymbol{\nabla} \times \mathbf{v}, \quad \langle \omega_y \rangle = \frac{\int d^3\mathbf{r}\ [\mathcal{W}(\mathbf{r})]\,\omega_y(\mathbf{r})}{\int d^3\mathbf{r}\ [\mathcal{W}(\mathbf{r})]}, \quad \mathcal{W}(\mathbf{r}) = \rho^2 \epsilon(\mathbf{r})$$

ρ: distance from y-axis

$\epsilon(\boldsymbol{r})$: energy density

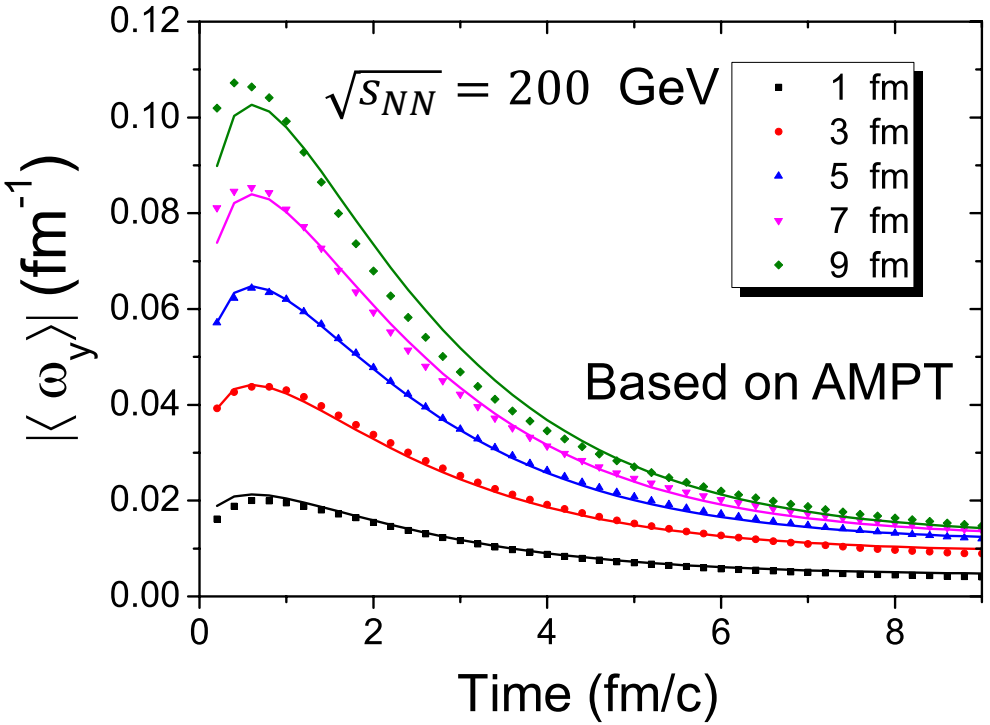

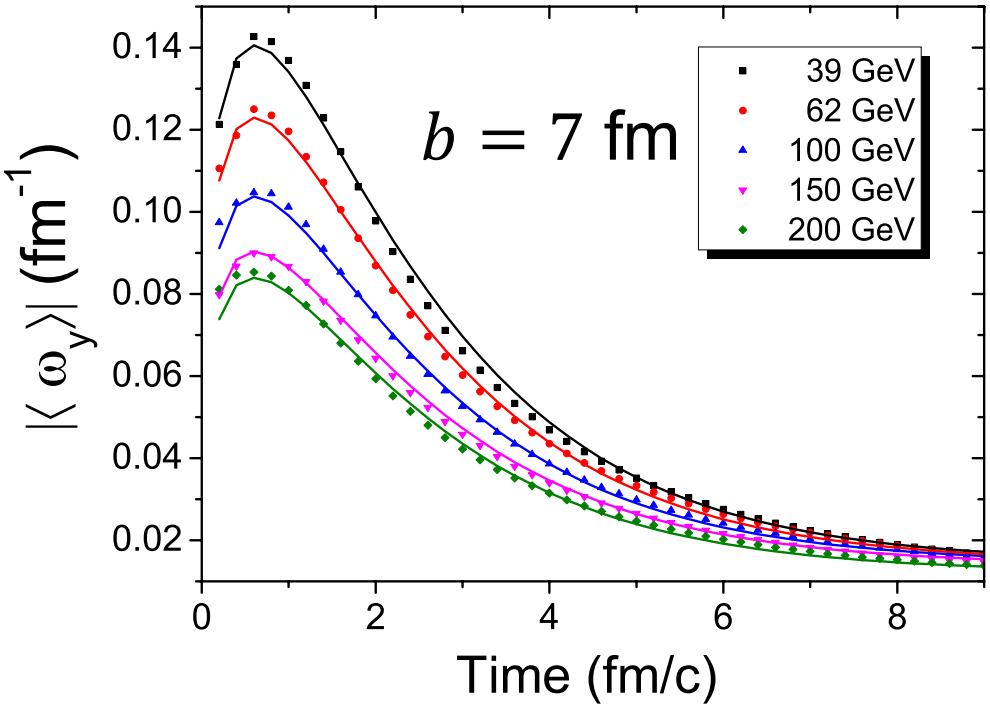

- Average vorticity decreases with time, decreasing impact parameter, and increasing collision energy. The lifetime is much longer than that of electromagnetic field.
- Can lead to chiral vortical effect and vortical separation effect

$$\mathbf{J}^V = \frac{\mu\mu_5}{\pi^2}\boldsymbol{\omega} \quad \text{and} \quad \mathbf{J}^A = \left(\frac{T^2}{6} + \frac{\mu^2 + \mu_5^2}{2\pi^2}\right)\boldsymbol{\omega}$$

Λ polarization in relativistic heavy ion collisions

- First suggested by Z. T. Liang & X. N. Wang, PRL 94, 102301 (2005)

Abelev (STAR), PRC 76, 024915 (2007)

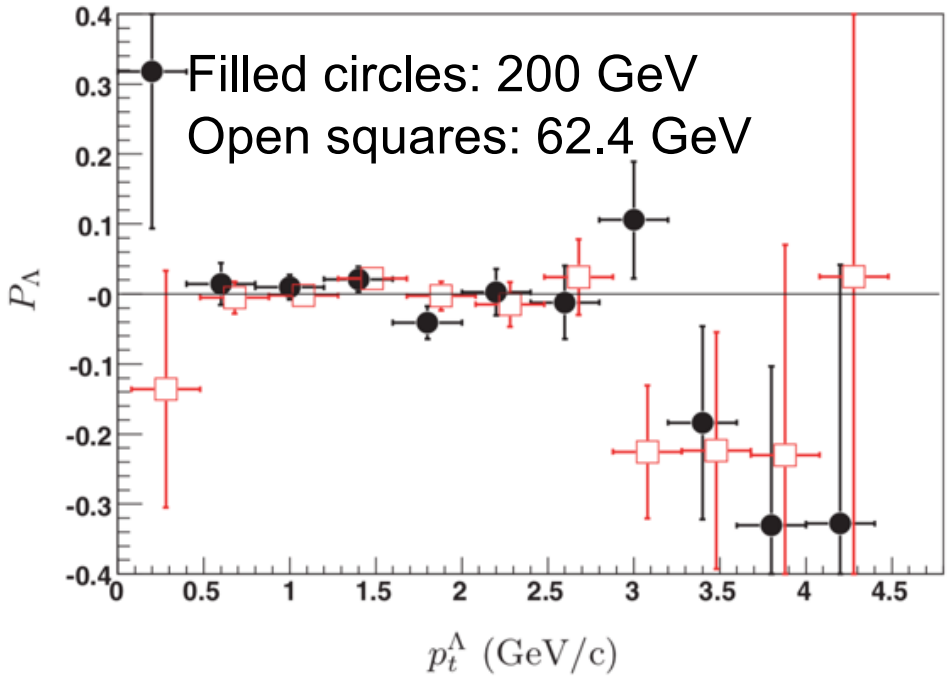

Adam (STAR), PRC 98, 14910 (2018)

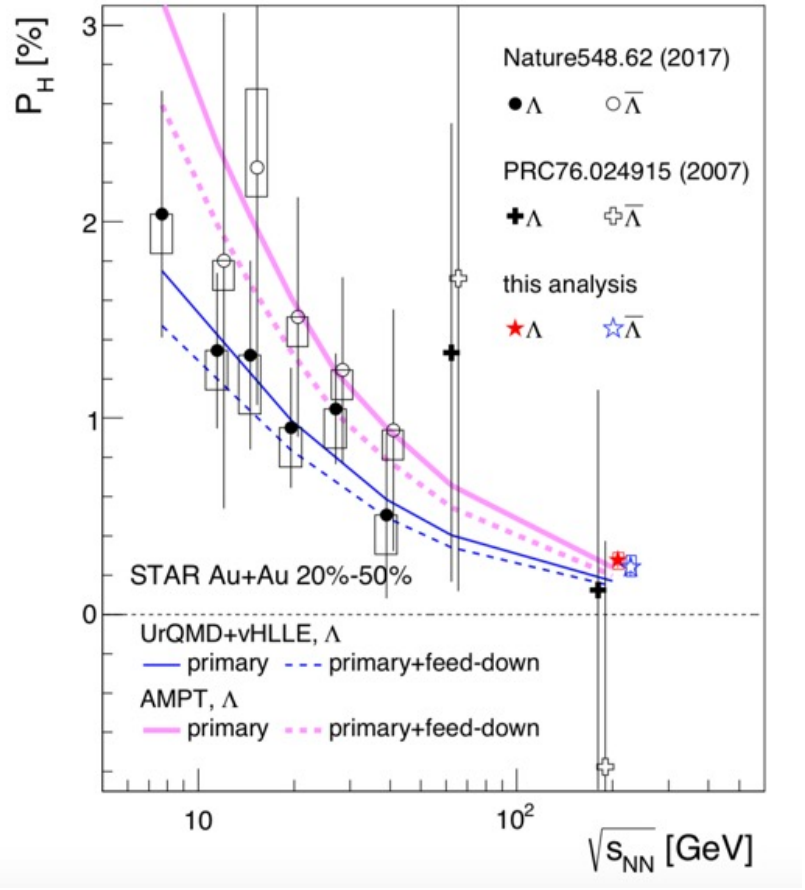

- Studies based on fluid dynamics [Cernai, Becatiini, Karpenko, Voloshin] and transport models [Wang et al.] assuming Λ in thermal equilibrium in the rotating fireball at chemical freeze out of HIC both predict Λ polarizations comparable to the STAR data.

Λ polarization from chiral kinetic approach

Sun & Ko, PRC 96, 024906 (2017)

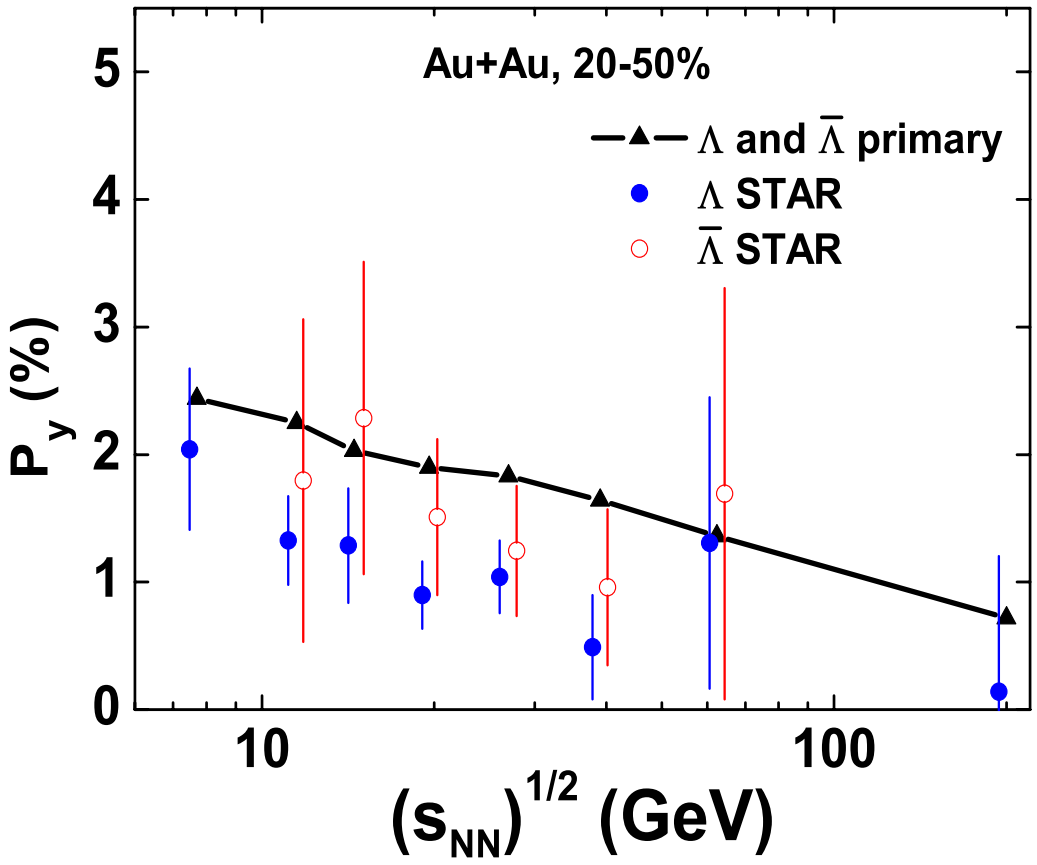

$$\frac{d\mathbf{x}}{dt} = \frac{\hat{\mathbf{p}} + 2\lambda|\mathbf{p}|(\hat{\mathbf{p}}\cdot\mathbf{b})\boldsymbol{\omega}}{1 + 6\lambda|\mathbf{p}|(\mathbf{b}\cdot\boldsymbol{\omega})}$$

$$\Lambda = \pm 1 = \text{helicity}$$

$$\mathbf{b} = \frac{\hat{\mathbf{p}}}{2|\mathbf{p}|^2} = \text{Berry curvature}$$

$$\frac{d\mathbf{p}}{dt} = 0$$

Including scattering that ensures the equilibrium distribution $\sqrt{G}f$ with $\sqrt{G} = 1 + 6\lambda|\mathbf{p}|(\mathbf{b}\cdot\boldsymbol{\omega})$.

- Consistent with data that Λ polarization decreases with collision energy due to decreasing vorticity field with increasing energy.

Exotic hadrons and their decay modes

ExHIC Collab: Cho, Furumoto, Hyodo, Jido, Ko, Lee, Nielsen, Ohnishi, Sekihara,Yasui, Yazaki, PRL 106, 212001 (2011); PRC 84, 064910 (2011), PPNP 95, 279 (2017).

Particle	m (MeV)	g	I	$J\pi$	$2q/3q/6q$	$4q/5q/8q$	Mol.	$\omega_{\rm Mol.}$ (MeV)	decay mode
T_{cc}^{1} †)	3797	3	0	1+	-	$qq\bar{c}\bar{c}$	$\bar{D}\bar{D}^*$	476(B)	$K^+\pi^- + K^+\pi^- + \pi^-$
T_{cb}^{0} †)	7123	1	0	0+	-	$qq\bar{c}\bar{b}$	$\bar{D}B$	128(B)	$K^+\pi^- + K^+\pi^-$
$D_s(2317)$	2317	1	0	0+	$c\bar{s}$ $(L=1)$	$q\bar{q}c\bar{s}$	DK	273(B)	$D_s\pi$ (strong decay)
$X(3872)$	3872	3	0	1+ *)	-	$q\bar{q}c\bar{c}$	$\bar{D}D^*$	3.6(B)	$J/\psi\pi\pi$ (strong decay)
$Z^+(4430)$ ‡)	4430	3	1	0− *)	-	$q\bar{q}c\bar{c}$ $(L=1)$	$D_1\bar{D}^*$	13.5(B)	$J/\psi\pi$ (strong decay)
$f_0(980)$	980	1	0	0+	$q\bar{q}, s\bar{s}$ $(L=1)$	$q\bar{q}s\bar{s}$	$\bar{K}K$	67.8(B)	$\pi\pi$ (strong decay)
$a_0(980)$	980	3	1	0+	$q\bar{q}$ $(L=1)$	$q\bar{q}s\bar{s}$	$\bar{K}K$	67.8(B)	$\eta\pi$ (strong decay)
$\Lambda(1405)$	1405	2	0	1/2−	qqs $(L=1)$	$qqqs\bar{q}$	$\bar{K}N$	20.5(R)−174(B)	$\pi\Sigma$ (strong decay)
$\Theta^+(1530)$ ‡)	1530	2	0	1/2+ *)	-	$qqqq\bar{s}$ $(L=1)$	-	-	KN (strong decay)
$\bar{K}KN$ †)	1920	4	1/2	1/2+	qqq	$qqqs\bar{s}$ $(L=1)$	$\bar{K}KN$	42(R)	$K\pi\Sigma$, $\pi\eta N$
Θ_{cs} †)	2980	4	1/2	1/2+	-	$qqqs\bar{c}$ $(L=1)$	-	-	$\Lambda + K^+\pi^-$
$\bar{D}N$ †)	2790	2	0	1/2−	-	$qqq\bar{q}c$	$\bar{D}N$	6.48(R)	$K^+\pi^-\pi^- + p$
BN †)	6200	2	0	1/2−	-	$qqq\bar{q}b$	BN	25.4(R)	$K^+\pi^-\pi^- + \pi^+ + p$
H †)	2245	1	0	0+	$qqqss$	-	ΞN	73.2(B)	$\Lambda\Lambda$ (strong decay)
$\bar{K}NN$ ‡)	2352	2	1/2	0− *)	$qqqqs$ $(L=1)$	$qqqqq\,s\bar{q}$	$\bar{K}NN$	20.5(T)-174(T)	ΛN (strong decay)
$\Omega\Omega$ †)	3228	1	0	0+	$ssssss$	-	$\Omega\Omega$	98.8(R)	$\Lambda K^- + \Lambda K^-$
H_c^{++} †)	3377	3	1	0+	$qqqsc$	-	$\Xi_c N$	187(B)	$\Lambda K^-\pi^+\pi^+ + p$
$\bar{D}NN$ †)	3734	2	1/2	0−	-	$qqqqq\,q\bar{c}$	$\bar{D}NN$	6.48(T)	$K^+\pi^- + d$, $K^+\pi^-\pi^- + p + p$
BNN †)	7147	2	1/2	0−	-	$qqqqq\,q\bar{b}$	BNN	25.4(T)	$K^+\pi^- + d$, $K^+\pi^- + p + p$

Exotic hadrons production in HIC

Coalescence / Statistical model ratio at RHIC

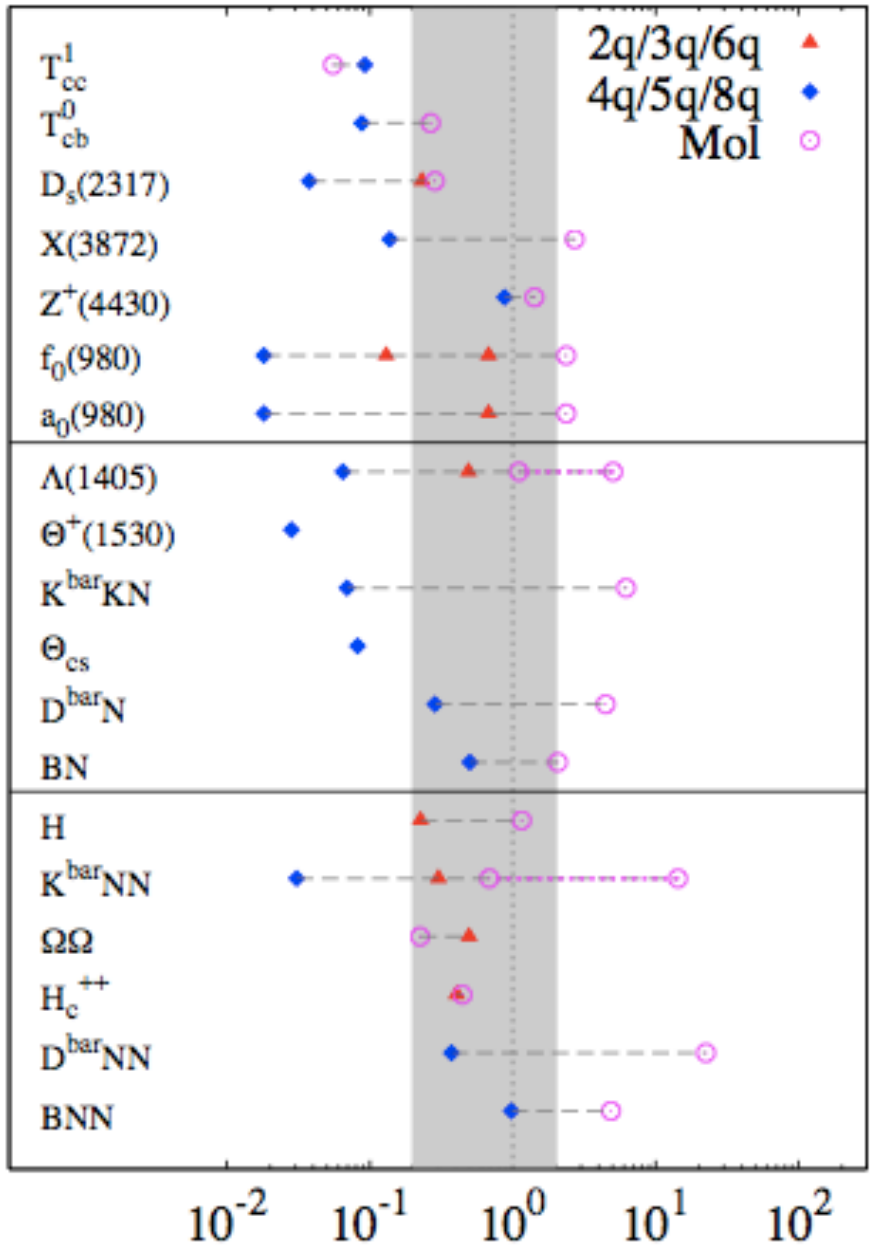

Coalescence / Statistical model ratio at LHC

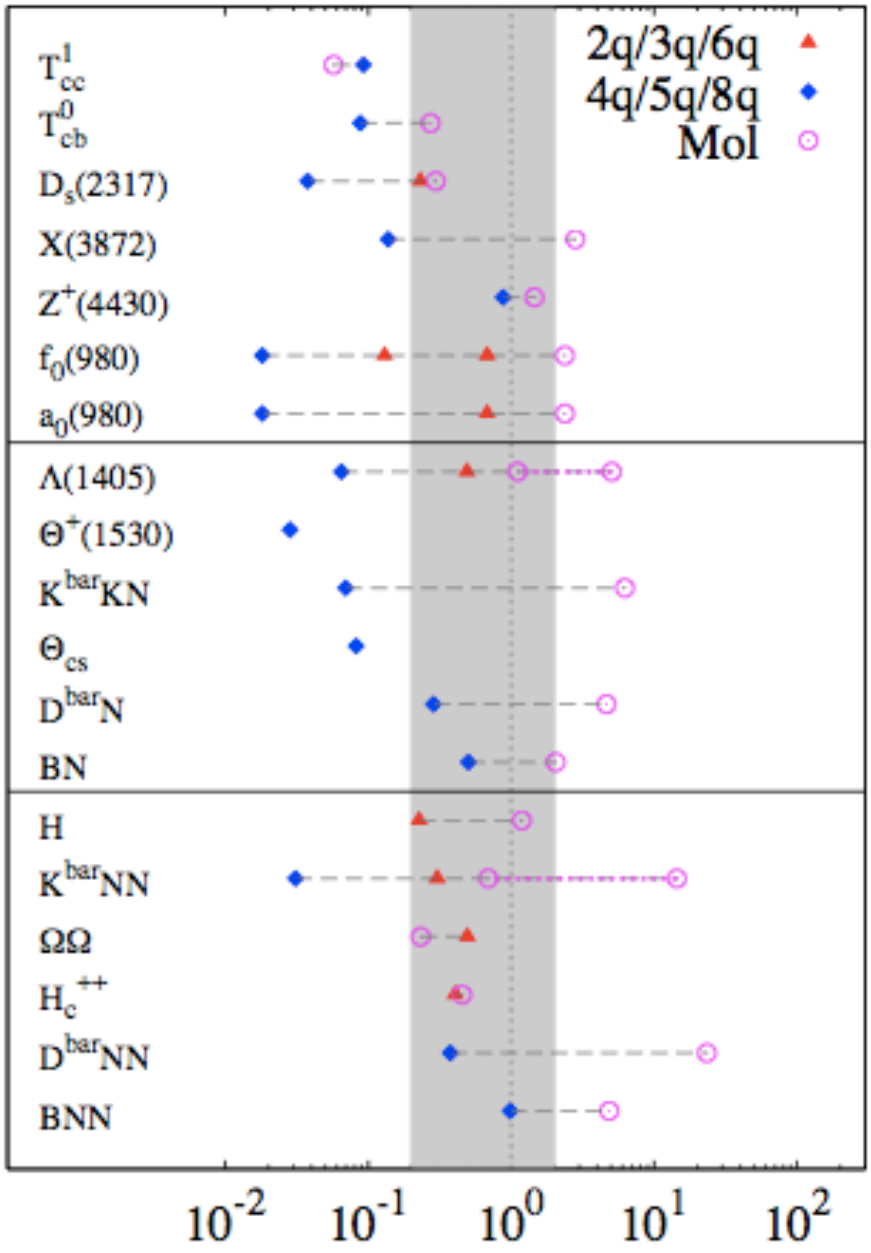

PHYSICAL REVIEW LETTERS **128,** 032001 (2022)

Evidence for X(3872) in Pb-Pb Collisions and Studies of its Prompt Production at $\sqrt{s_{NN}} = 5.02$ TeV

A. M. Sirunyan *et al.*[*]
CMS Collaboration

The first evidence for X(3872) production in relativistic heavy ion collisions is reported. The X(3872) production is studied in lead-lead (Pb-Pb) collisions at a center-of-mass energy of $\sqrt{s_{\mathrm{NN}}} = 5.02$ TeV per nucleon pair, using the decay chain $\mathrm{X}(3872) \to J/\psi\pi^+\pi^- \to \mu^+\mu^-\pi^+\pi^-$. The data were recorded with the CMS detector in 2018 and correspond to an integrated luminosity of 1.7 nb^{-1}. The measurement is performed in the rapidity and transverse momentum ranges $|y| < 1.6$ and $15 < p_{\mathrm{T}} < 50$ GeV/c. The significance of the inclusive X(3872) signal is 4.2 standard deviations. The prompt X(3872) to $\psi 2S$ yield ratio is found to be $\rho^{\mathrm{Pb\text{-}Pb}} = 1.08 \pm 0.49(\mathrm{stat}) \pm 0.52(\mathrm{syst})$, to be compared with typical values of 0.1 for pp collisions. This result provides a unique experimental input to theoretical models of the X(3872) production mechanism, and of the nature of this exotic state.

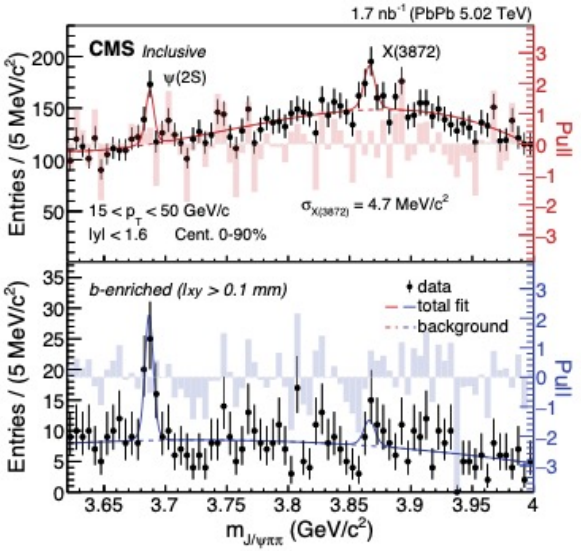

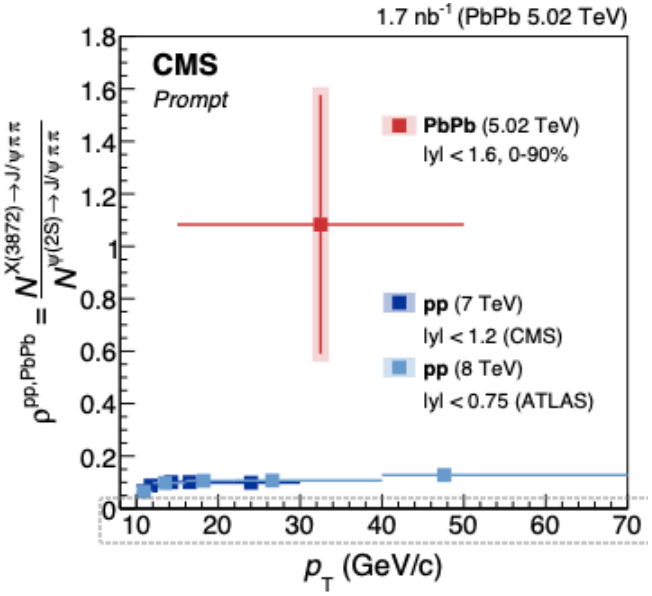

$$\frac{X(3872)}{\psi(2S)} \approx 1$$

which is a factor of ten larger than in p+p collisions

X(3872) production in HIC

Cho & Lee, PRC 88, 054901 (2013)

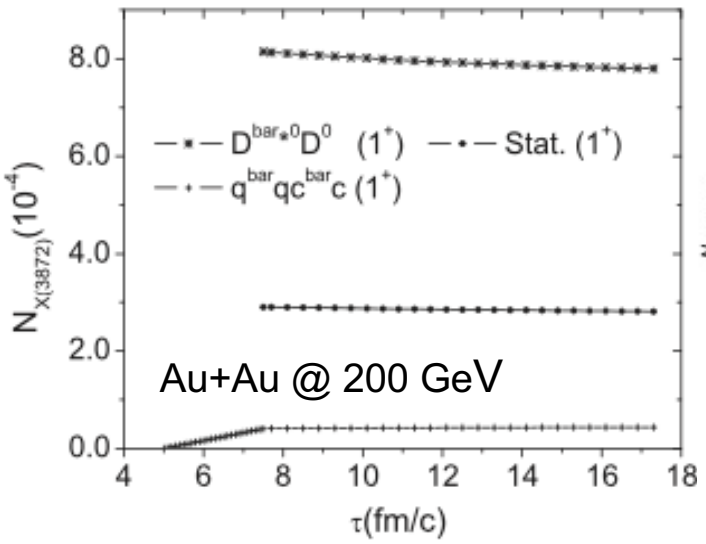

Abreu et al., PLB 761, 303 (2016)

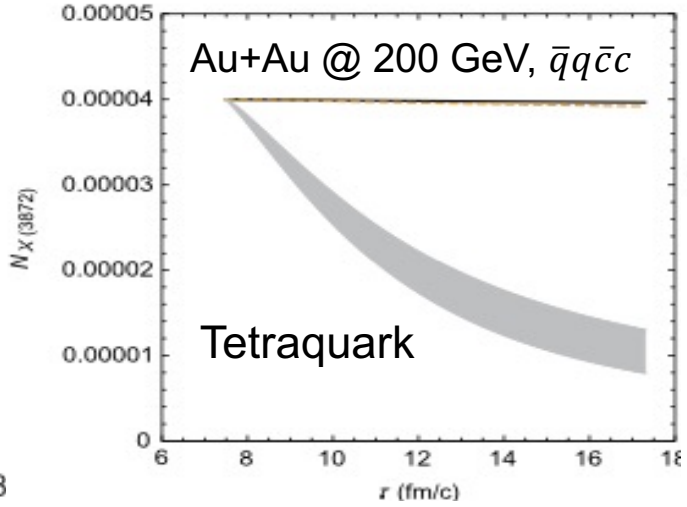

Wu, Du, Sibila & Rapp, EPJA 57, 122 (2021)

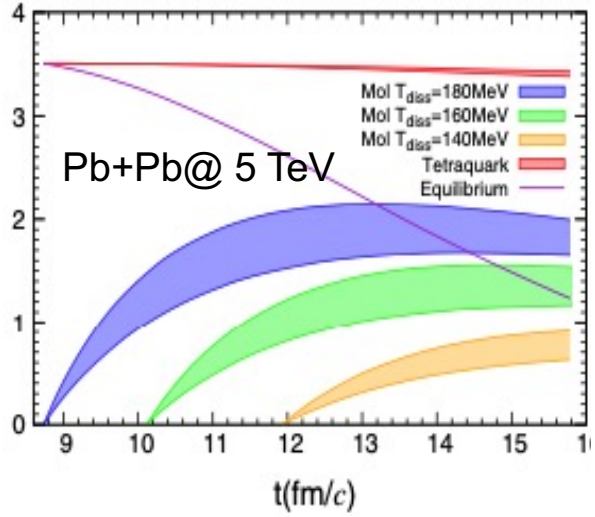

Hui Zhang et al, PRL 126, 012301 (2021)

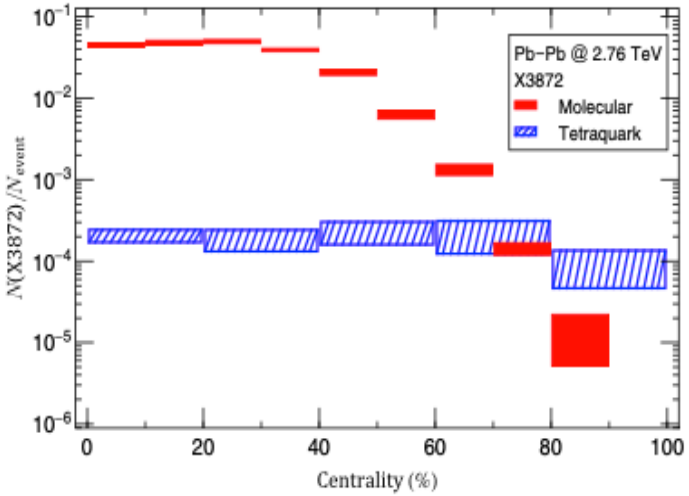

- Cho & Lee use kinetic approach with initial numbers from coalescence model and include $\pi(\rho)X \leftrightarrow D\bar{D}, D^*\bar{D}, D^*\bar{D}^*$ reactions.
- Abreu et al. include anomalous vertices in $\pi X \leftrightarrow D\bar{D}, D^*\bar{D}, D^*\bar{D}^*$, resulting in larger cross sections.
- Wu et al. use thermal model for initial number and assume smaller cross sections for tetraquark scenario. Molecular X(3872) is produced from hadronic reactions.
- Zhang et al. use $D\bar{D}$ coalescence for molecular scenario and diquark-diquark coalescence for tetraquark scenario based only on their spatial distributions from AMPT.

Determination of the Neutron Skin of ^{208}Pb from Ultrarelativistic Nuclear Collisions

Giuliano Giacalone, Govert Nijs & Wilke van der Schee, PRL 131, 202302 (2023)

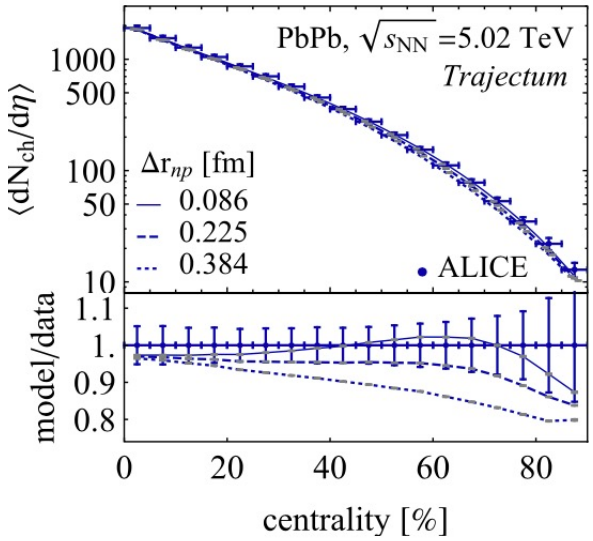

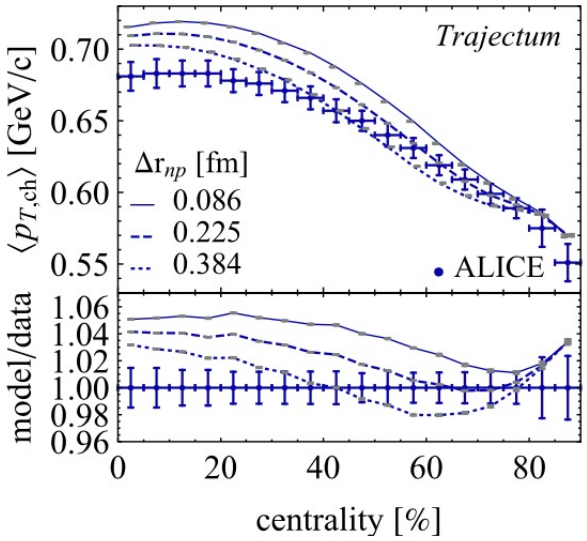

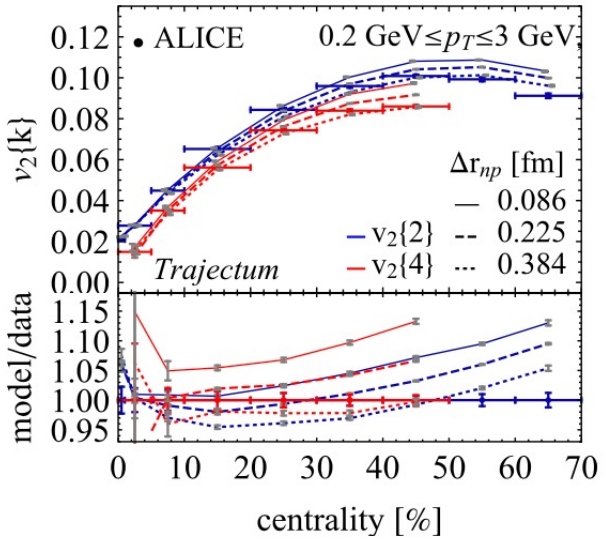

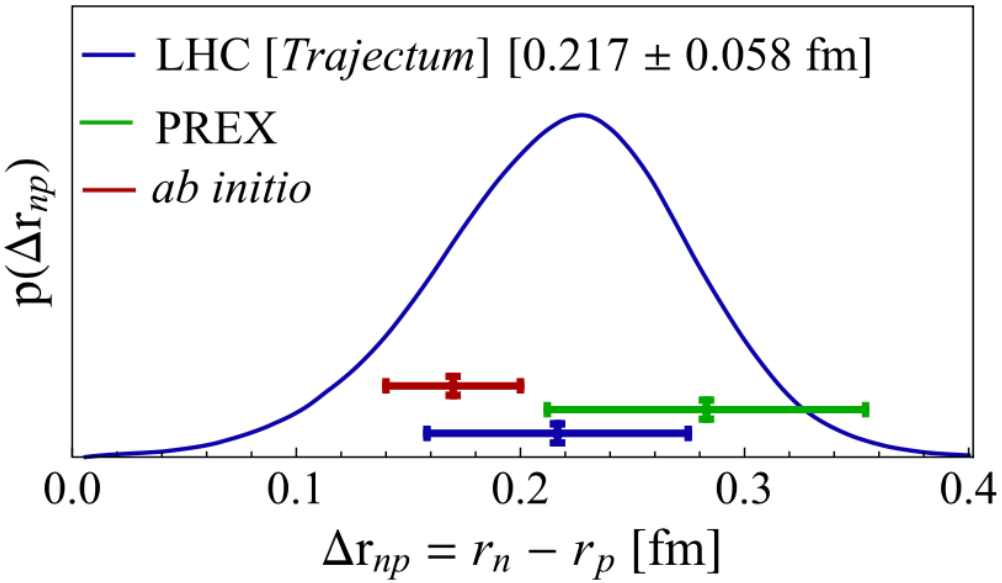

- A new experimental method to systematically measure neutron distributions in the ground state of atomic nuclei.
- Other studies have also shown the possibility to study nuclear deformations in relativistic heavy ion collisions. [Giacalone, Jianyong Jia, Fuqiang Wang, ….]

Conclusions

- Heavy ion collisions have made it possible to learn about the properties of strong-interaction matter matter
  - Low energies → strong dissipation of ~ 15 MeV/fm in nuclear collective motion
  - High energies → isoscalar incompressibility K~ 210-300 MeV
  - With neutron-rich nuclei → $E_{sym}(\rho) \sim 32\,(\rho/\rho_0)^{\gamma}$ with $0.7<\gamma<1.1$

    for $\rho < 1.2\rho_0 \rightarrow K_{asy}(\rho_0) \sim -550 \pm 50$ MeV and $L \sim 88 \pm 25$ (55 ± 18)
  - Relativistic energies → a strongly coupled quark-gluon plasma
- Future radioactive beam facilities → Nuclear symmetry energy at high densities
- Experiments at LHC and future FAIR allow to probe QGP at even higher temperature and finite baryon chemical potential, respectively
- LHC → charm exotics and information on nuclear structure